

## Overview

|  |     |
|--|-----|
| 1 Abbreviations .....  | III |
| 2 Acknowledgements .....   | V   |
| 3 Abstract .....   | VII |
| 4 Samenvatting .....   | IX  |
| 5 Introduction .....   | 11  |
| 5.1 Multiple sclerosis.....  | 11  |
| 5.2 CD4+CD28null T cells.....  | 12  |
| 5.3 Chronic stimulation .....  | 14  |
| 5.4 Aim of this study.....   | 15  |
| 6 Materials and methods .....  | 17  |
| 6.1 Identification of CD4+CD28null T cells by means of flow cytometry .....            | 17  |
| 6.2 CMV assay .....  | 17  |
| 6.3 Stimulation of MBP specific T cell clones with MBP and PHA .....                   | 18  |
| 6.4 Optimization of the differentiation assay .....                                    | 18  |
| 6.4.1 Standard polymerase chain reaction .....   | 18  |
| 6.4.2 Sequencing PCR .....   | 18  |
| 6.4.3 Differentiation assay using cytokine cocktail .....                              | 18  |
| 6.5 EAE mouse model .....  | 20  |
| 6.5.1 Immunization.....  | 20  |
| 6.5.2 Isolation of cells .....   | 21  |
| 6.5.3 Identification of CD4+CD28null T cells .....                                     | 22  |
| 6.5.4 Immunohistochemistry.....  | 22  |
| 6.6 Statistics.....  | 22  |
| 7 Results.....   | 23  |
| 7.1 Percentage of CD4+CD28null T cell expansion in MS and HC donors.....               | 23  |
| 7.2 <i>In vitro</i> stimulation of MBP specific T cell clones with MBP and PHA .....   | 23  |
| 7.3 <i>In vitro</i> proliferation of CD4+CD28null T cells by means of CMV assays ..... | 24  |
| 7.2 Differentiating capacities of CD4+CD28null T cells.....                            | 28  |
| 7.2.1 Functionality of primers.....  | 28  |
| 7.2.2 Gene expression after differentiation cocktails.....                             | 29  |
| 7.3 EAE study to determine the <i>in vivo</i> presence of CD4+CD28null T cells .....   | 31  |
| 8 Discussion .....   | 37  |

|   |    |
|---|----|
| 9 References.....                         | 45 |
| 10 Supplementary figures and tables ..... | 49 |

# 1 Abbreviations

|                                |  |
|--------------------------------|--|
| <b>BBB</b>                     | blood-brain-barrier  |
| <b>Bcl-2</b>                   | B-cell lymphoma 2  |
| <b>CCR7</b>                    | chemokine receptor type 7  |
| <b>CD</b>                      | cluster of differentiation   |
| <b>CD127</b>                   | interleukin-7 receptor alpha   |
| <b>CD62L</b>                   | L-selectin   |
| <b>CFA</b>                     | complete Freund's adjuvant   |
| <b>CMV</b>                     | cytomegalovirus  |
| <b>CMV-/Exp-</b>               | cytomegalovirus seronegative donor without CD4+CD28null T cell expansion |
| <b>CMV+/Exp-</b>               | cytomegalovirus seropositive donor without CD4+CD28null T cell expansion |
| <b>CMV+/Exp+</b>               | cytomegalovirus seropositive donor with CD4+CD28null T cell expansion    |
| <b>CNS</b>                     | central nervous system   |
| <b>CX<sub>3</sub>CR1</b>       | fractalkine receptor   |
| <b>DAPI</b>                    | 4',6-diamidino-2-phenylindole  |
| <b>EAE</b>                     | experimental autoimmune encephalomyelitis                                |
| <b>EDTA</b>                    | ethylenediaminetetraacetic acid  |
| <b>FBS</b>                     | fetal bovine serum   |
| <b>FLICE</b>                   | Fas-associated death domain-like IL-1-converting enzyme                  |
| <b>FLIP</b>                    | FLICE- like inhibitory protein   |
| <b>GATA-3</b>                  | Trans-acting T-cell-specific transcription factor                        |
| <b>HEPES</b>                   | 4-(2-hydroxyethyl)-1-piperazineethanesulfonic acid                       |
| <b>IFN</b>                     | interferon   |
| <b>IL</b>                      | interleukin  |
| <b>LFA-1</b>                   | lymphocyte function-associated antigen 1                                 |
| <b>MBP</b>                     | myelin basic protein   |
| <b>MHC</b>                     | major histocompatibility complex   |
| <b>MicB</b>                    | MHC class I polypeptide-related sequence B                               |
| <b>MOG</b>                     | myelin oligodendrocyte glycoprotein                                      |
| <b>MRI</b>                     | magnetic resonance imaging   |
| <b>MS</b>                      | multiple sclerosis   |
| <b>NCAM/CD56</b>               | neural cell adhesion molecule  |
| <b>NKG2D</b>                   | natural killer group 2, member D   |
| <b>PBMC</b>                    | peripheral blood mononuclear cell  |
| <b>PBS</b>                     | phosphate buffered saline  |
| <b>PCR</b>                     | polymerase chain reaction  |
| <b>PFA</b>                     | paraformaldehyde   |
| <b>PHA</b>                     | phytohemagglutinin   |
| <b>PTX</b>                     | pertussis toxin  |
| <b>qPCR</b>                    | real time polymerase chain reaction                                      |
| <b>ROR<math>\gamma</math>T</b> | RAR-related orphan receptor gamma T                                      |
| <b>SNP</b>                     | single nucleotide polymorphism   |
| <b>T-bet</b>                   | T-box transcription factor TBX21   |
| <b>Th</b>                      | T helper cell  |
| <b>TLR-2</b>                   | toll-like receptor 2   |
| <b>TNF-<math>\alpha</math></b> | tumor necrosis factor alpha  |
| <b>VLA-4</b>                   | very late antigen 4  |



## **2 Acknowledgements**

For the past 8 months I have been working on my senior internship. During this internship I have experienced some ups and downs. This project would not have been the same without the help and support of several people. Therefore there are many people I would like to thank.

First of all I would like to thank my promotor Prof. dr. Niels Hellings and co-promotor dr. Liesbet Peeters for giving me the opportunity to perform this study at the biomedical research institute (BIOMED). Furthermore I would like to thank them and the other members of the immunology group for their critical view on my senior project, which has led to a better end result of this study and has helped me further developing my researching skills.

Next, many thanks to Marjan Vanheusden, who has guided me throughout this project and has helped me achieve my goals. Many thanks for reading and evaluating my senior thesis.

Moreover, I would like to thank Christel Bocken and Katrien Wauterickx for their help in the laboratory when problems arose. Furthermore, many thanks to my second examiner dr. Judith Fraussen for the helpful discussion concerning my senior project.

Also a word of appreciation for Lindsey Wanten, and Liesbeth Indesteege who both assisted me during some of the experiments performed in this project.

At last many thanks to my fellow students for their support in difficult times, and for all the laughs and unforgettable times in the student's room.



### 3 Abstract

**Introduction:** Multiple sclerosis (MS) is an autoimmune disease characterized by autoreactive T cells destroying myelin, and oligodendrocytes. Several autoreactive immune cells are known that could contribute to MS pathology. In this study the origin and the contribution of CD4+CD28null T cells, a T cell subset lacking the CD28 costimulatory molecule, to MS pathology will be investigated. CD4+CD28null T cells are thought to originate due to chronic inflammation, and in specific chronic CMV stimulation. CMV belongs to the family of betaherpesviruses, and is a latent virus. This means that once infected, this virus persists throughout life.

The CD4+CD28null T cell subset exhibits several cytotoxic properties, including a high production of IFN- $\gamma$  and granzyme B, they have an upregulation of many adhesion molecules that can facilitate their invasion in MS lesions, and their proliferation could not be suppressed by regulatory T cells. These properties suggest that they can contribute to MS pathology.

**Materials and methods:** The autoreactivity of CD4+CD28null T cells was determined by chronically stimulating MBP specific T cell clones with MBP and PHA.

The origin and expansion of these cells was investigated by co-culturing CD4+CD28null T cells with autologous irradiated feeder cells, which were pulsed with CMV pp65 with or without supplementing IL-2.

A Th differentiation assay was optimized, in which a co-culture of CD4+CD45RO+ T cells and CD14+ cells were stimulated with Th1, Th2, or Th17 specific cytokines. Gene expression of Th1, Th2, and Th17 genes were measured by means of qPCR.

Furthermore the presence of these cells was investigated in the peripheral blood and several organs (lymph nodes, spleen, brain, and spinal cord) an *in vivo* EAE model (n=25), also their possible role in aggravating EAE pathology was determined. Immunohistochemical stainings were optimized to stain for CD4+CD28null T cells in the spinal cord, by means of CX<sub>3</sub>CR1, CD4, and CD3 staining.

**Results:** Data from this study demonstrates that the CD4+CD28null T cell fraction in MBP specific T cells increases after several stimulation rounds with MPB and PHA.

Furthermore this study shows that the percentage of CD4+CD28null T cells increases in a CMV stimulatory environment in a CMV seropositive donor with an already present CD4+CD28null T cell expansion.

Moreover this study provides evidence for the presence of the CD4+CD28null T cell subset in an EAE model, and a correlation between this cell percentage and EAE score is found.

**Conclusion:** This study shows that a proportion of CD4+CD28null T cells are autoreactive. The CD4+CD28null T cell subset is reactive towards CMV, and their origin may be caused by chronic CMV stimulation.

Moreover CD4+CD28null T cells are present in an EAE mouse model, and aggravate EAE.



## 4 Samenvatting

**Introductie:** Multiple sclerosis (MS) is een auto-immune aandoening die gekarakteriseerd wordt door auto-reactieve T cellen die myeline en oligodendrocyten afbreekt. Verschillende auto-reactieve immuun cellen die een rol kunnen spelen in MS pathologie zijn gekend. In deze studie worden de oorsprong en de bijdrage van CD4+CD28null T cellen, een specifieke T cel populatie waarvan het CD28 co-stimulatorische molecuule ontbreekt, aan MS pathologie onderzocht. De oorsprong van de CD4+CD28null T cellen wordt gedacht zich te bevinden in chronische inflammatie, en in het specifiek chronische CMV stimulatie. CMV behoort tot de betaherpes virus familie, en is een latente virus. Dit betekent dat eens iemand geïnfecteerd is, het virus gedurende heel het leven aanwezig blijft.

De CD4+CD28null T cellen hebben verschillende cytotoxische eigenschappen, zoals een verhoogde IFN- $\gamma$  en granzyme B productie. Ze hebben een verhoging van veel adhesie moleculen die hun invasie in MS laesies kan vergemakkelijken. Hun proliferatie kan ook niet onderdrukt worden door regulatoire T cellen. Deze verschillende eigenschappen tonen aan dat de CD4+CD28null T cellen kunnen bijdragen aan MS pathologie. Verder zal de aanwezigheid van deze cellen onderzocht worden in een *in vivo* EAE model.

**Materiaal en methoden:** De autoreactiviteit van de CD4+CD28null T cellen werd bepaald door MBP specifieke T cel klonen chronisch te stimuleren met MBP en PHA.

De oorsprong van deze cellen werd bepaald door een co-cultuur van de CD4+CD28null T cellen met autologe bestraalde cellen bloot te stellen aan CMV pp65 stimulatie samen of zonder IL-2 toevoeging. Een Th differentiatie assay werd geoptimaliseerd, waarin een co-cultuur van CD4+CD45RO+ T cellen en CD14+ cellen gestimuleerd werden met Th1, Th2, of Th17 specifieke cytokines. Gen expressie van Th1, Th2, en Th17 genen werd bepaald door gebruik te maken van qPCR.

Verder werd de aanwezigheid van deze cellen in het perifere bloed en verschillende organen (lymfe knopen, milt, hersenen, en ruggenmerg) in een *in vivo* EAE model (n=25) bepaald, ook werd de rol van de CD4+CD28null T cellen in de verergering van EAE onderzocht. Immunohistochemische kleuringen werden geoptimaliseerd om CD4+CD28null T cellen aan te kleuren in het ruggenmerg, door middel van CX<sub>3</sub>CR1, CD4, en CD3 kleuringen.

**Resultaten:** Data uit deze studie toont aan dat de CD4+CD28null T cel fractie in MBP specifieke T cellen stijgt na enkele stimulatie ronden met MBP en PHA.

Verder toont deze studie aan dat het CD4+CD28null T cel percentage stijgt in een CMV stimulatorische omgeving in een CMV seropositieve donor met al een aanwezige CD4+CD28null T cel expansie.

Deze studie leverde bewijs voor de aanwezigheid van de CD4+CD28null T cellen in een EAE model, ook werd een correlatie tussen CD4+CD28null T cel percentage en EAE score gevonden.

**Conclusie:** Deze studie toont dat een deel van de CD4+CD28null T cellen autoreactief zijn. CD4+CD28null T cellen zijn reactief tegen CMV, en hun oorsprong kan veroorzaakt worden door chronische CMV stimulatie.

CD4+CD28null T cellen zijn aanwezig in een EAE muis model, en verergeren het ziekteverloop van EAE.



## 5 Introduction

### 5.1 Multiple sclerosis

Multiple sclerosis (MS) is an autoimmune disease characterized by autoreactive immune cells, such as lymphocytes and macrophages, destroying cells and tissues, namely oligodendrocytes and myelin (1). Oligodendrocytes are cells responsible for the production of myelin and wrapping the myelin around the axons of the central nervous system (CNS). Myelin is a substance that improves the conductance of the electrical signals which pass through these axons. When myelin gets damaged or progressively declines, the conductivity of the electrical signals passing through the axons will decrease (2). This will eventually lead to several symptoms including fatigue, weakening of muscles, cognitive impairment, and ataxia (1). The pathogenesis of MS starts with increased migration of autoreactive T lymphocytes, through the blood brain barrier (BBB). Normally the BBB prevents immune cells from reaching the CNS, but in MS the BBB is more permeable. This permeable state could be caused by various proinflammatory cytokines (e.g. IFN- $\gamma$ , TNF- $\alpha$ ) released by the immune cells (3). When regulatory lymphocytes fail to suppress the autoreactive T lymphocytes that cross the BBB, immune responses in the brain can be induced. Increasing numbers of these autoreactive immune cells will lead to a higher production of proinflammatory cytokines that attracts other immune cells, and will lead to the breakdown of myelin, which are seen as the plaques in the brain on magnetic resonance imaging (MRI) in MS patients (1, 4). Currently, there are two hypotheses that explain the epidemiology of MS. The hygiene hypothesis states that a virus acquired early in life (infancy) will diminish the chance of developing MS than if the same virus was acquired late in life (late adulthood or childhood)(1, 5). The prevalence hypothesis states that a pathogen present in a high prevalence MS region is the cause of MS, only in some cases and after many years can this pathogen cause MS (5).

MS is a relatively common autoimmune disease. In 2013, the worldwide the median prevalence of MS was estimated to be 33 cases per 100.000 inhabitants. In North America the highest median prevalence of MS in the world is found, being 140 cases per 100.000 inhabitants (6). Regarding the median incidence of MS in 2008, worldwide it was estimated to be 2.5 cases per 100.000 inhabitants. The highest median incidence can be found in Europe, being 3.8 cases per 100.000 inhabitants (7). MS often strikes relatively young adults, worldwide the average onset of MS is estimated to be 29.2 years. Women are usually more at risk to develop MS, worldwide the median female to male ratio is estimated to be 2:1. In South-East Asia the highest median female to male ratio can be found, which is 3:1 (6, 7).

Both environmental factors (such as infections and geography) as well as genetic factors (such as the human leukocyte antigen molecules DQ6 and DR15) are suggested to play a role in this disease (1), which emphasizes the complexity of MS.

The diagnosis of MS is mainly based on the McDonald criteria together with neuroimaging tools such as MRI. The McDonald criteria list the data that is needed to diagnose a person with MS after they show themselves with a certain clinical presentation. This is done by showing a dissemination of brain

lesions in space and time (1, 8, 9). MRI can be used to show the demyelination (brain lesions) that is occurring in MS, since MRI uses gadolinium as contrast agent that normally cannot cross the BBB. Multiple clinical courses of MS exist. 80% of MS patients initially have a clinically isolated syndrome, which is an episode affecting one site. Some of these patients enter a relapsing remitting form of MS; these patients develop symptoms that remain present for a certain amount of time before disappearing again. Relapsing remitting MS patients do not recover completely after a relapse, eventually leading to persistent symptoms. 65% of these patients develop the secondary progressive phase, in which patients do not show any recovery after an episode. 20% of MS patients enter this progressive phase from the onset of disease, these patients are primary progressive (1). A minority of patients (approximately 5%) have a form of MS that is progressive from onset of disease and on top of that has superimposed relapses, this form of MS is called progressive relapsing (10).

Up to now MS still is incurable. Current treatments try to reduce the relapses and the progression of the disease in relapsing remitting and secondary progressive MS patients. To date most treatments are directed against the relapsing remitting form of MS, there are only a few treatments for the secondary progressive form of MS. Examples of treatments for relapsing remitting MS patients are Avonex, Rebif, Betaferon, which all work through the active ingredient interferon  $\beta$  (IFN- $\beta$ ) (11-14). These treatments are considered first line treatments. IFN- $\beta$  influences the aberrant immune activity seen in MS by decreasing class II major histocompatibility complex (MHC) molecules, by lowering the migration of immune cells across the BBB, and by decreasing elevated T-cell derived cytokines such as IFN- $\gamma$ , and TNF- $\alpha$  (12).

Another example of a first-line treatment for relapsing remitting MS patients is Copaxone, with glatiramer acetate as active component (15). Glatiramer acetate inhibits the activation of MBP reactive T cells and generates T-cells which have anti-inflammatory properties (13, 14).

An example of a second-line treatment for relapsing remitting MS patients include fingolimod, which limits the egression of lymphocytes from secondary lymphoid tissues into the blood and thus decreases the amount of lymphocytes crossing the BBB (16, 17).

Mitoxantrone is an example of one of the few treatments used in secondary progressive MS patients and in patients who do not respond to other treatments. Mitoxantrone prevents DNA from replicating and creates single and double strand breaks by intercalating in DNA. This treatment however cannot be administered for a longer duration than 2-3 years due to its severe side effects such as cardiotoxicity and acute myeloid leukemia, which is why it is not a first line treatment (18).

## **5.2 CD4+CD28null T cells**

There are many immune cells known that contribute to the pathology of MS. In this study the contribution of CD4+CD28null T cells, a sub-population of T cells lacking the expression of the CD28 co-stimulatory molecule, to the pathology of MS will be investigated. Normally the CD28 co-stimulatory molecule is necessary for T cells to induce an immune response. However, the CD4+CD28null T cells appear to make an exception, since they are still able to generate an immune response despite losing the CD28 co-stimulatory molecule (19-21). This implicates that this T cell subset has become independent of co-stimulation.

The CD4+CD28null T cells also have been described to have enhanced cytotoxic capacities; they show high levels of effector molecules such as granzymes and perforin (20-24), they produce large amounts of IFN- $\gamma$  (21, 24-26), and display natural killer cell like receptors (e.g. killer-cell immunoglobulin-like receptor and NKG2D) (20-24, 26, 27). A subset of CD4+CD28null T cells are suggested to be autoreactive as they showed an increased proliferation towards auto-antigens, and increased levels of these cells are found in some MS patients (19, 23, 28). Another finding that suggests an autoreactive role of CD4+CD28null T cells is that an increase of these cells is found in other chronic inflammatory diseases, such as rheumatoid arthritis, Wegener's granulomatosis, Graves' disease (22, 23, 28).

CD4+CD28null T cells have certain upregulated adhesion molecules, which could increase their infiltration into sites of inflammation. For instance they have an increased expression of lymphocyte function-associated antigen 1 (LFA-1), neural cell adhesion molecule (NCAM or CD56), very late antigen-4 (VLA-4), which are important in the recruitment to the site of infection (22, 25, 29), cell-cell adhesion (27), and penetrating the BBB (25, 27).

CD4+CD28null T cells also have an upregulation of the fractalkine receptor (CX<sub>3</sub>CR1), which is a chemokine receptor. The expression of CX<sub>3</sub>CR1 is limited to the CD4+CD28null T cell subset, when compared to CD4+CD28+ T cells. Fractalkine is the ligand of this receptor, which is upregulated in the cerebrospinal fluid of MS patients. CD4+CX<sub>3</sub>CR1+ cells were found inside active lesions of MS patients (27).

The CD4+CD28null T cell subset has some downregulated molecules. A downregulation of C-C chemokine receptor type 7 (CCR7) (22), interleukin-7 receptor- $\alpha$  (CD127) (27), and L-selectin (CD62L) (27) has been reported. These adhesion molecules play a role as homing receptors to secondary lymphoid organs, and the development of immune cells.

The upregulation and downregulation of certain adhesion molecules on CD4+CD28null T cells suggests that these cells move to sites of inflammation and even active MS lesions and may play a role there. These markers indicate that CD4+CD28null T cells have an effector memory T cell phenotype.

The main changes in phenotype between CD4+CD28+ T cells and CD4+CD28null T cells with respect to receptors, granules and cytokines are depicted in figure 1.

Research also has shown that the proliferation of CD4+CD28null T cells could not be suppressed by regulatory T cells. The reason for this is because regulatory T cells control proliferation by taking transcriptional control of IL-2, and since CD4+CD28null T cells are IL-2 deficient cells their proliferation cannot be controlled (28). Another property of CD4+CD28null T cells is that they are very resistant to apoptosis (20), since they have an upregulation of the anti-apoptotic molecules B-cell lymphoma 2 (Bcl-2) (23, 30), FLICE-like inhibitory protein (FLIP) (23, 30), and a dysregulation of FLICE (24).

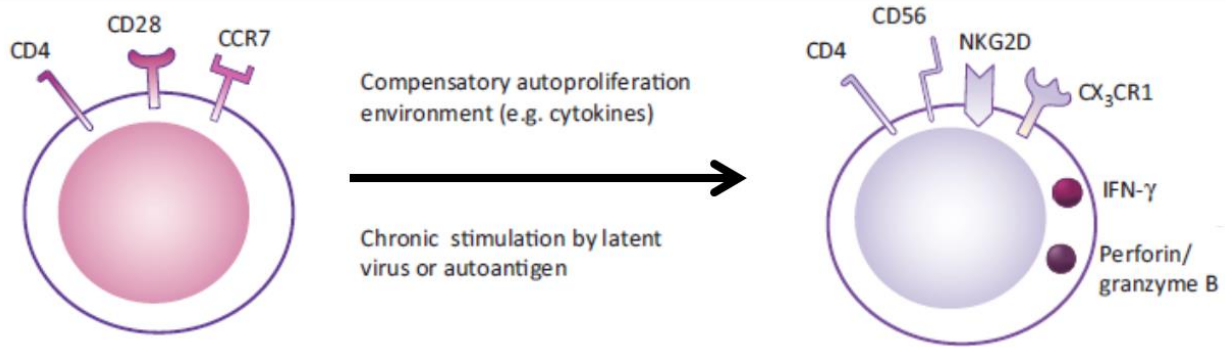


**Figure 1: Molecular changes after transition from CD4+CD28+ T cell to CD4+CD28null T cell.**

The left side of the figure shows a CD4+CD28+ T cell. After chronic stimulation by a latent virus or in a proinflammatory environment CD4+CD28+ T cells gradually lose their CD28 co-stimulatory molecule. They also lose the C-C chemokine receptor type 7 (CCR7) receptor and gain receptors such as neural cell adhesion molecule (CD56), NKG2D, and the fractalkine receptor (CX<sub>3</sub>CR1). Next to the upregulation of receptors they also gain cytotoxic granules and cytokines such as IFN- $\gamma$ , perforin, and granzyme B.

The increased cytotoxic capacities, upregulation and downregulation of certain adhesion molecules and in specific migration to active MS lesions, resistance to proliferation inhibition by regulatory T cells, a subset suggested to be autoreactive, and resistance to apoptosis of the CD4+CD28null T cells as discussed above enables these cells to be a harmful cell subset in the pathology of MS.

### 5.3 Chronic stimulation

As mentioned in section 5.2 the CD4+CD28null T cells lack the CD28 co-stimulatory molecule. This may be attributed to several factors. First of all the loss of CD28 is suggested to be caused by pro-inflammatory cytokines, such as tumor necrosis factor- $\alpha$  (TNF- $\alpha$ ), interleukin (IL) -2, IL-7, IL-15, IFN- $\alpha$  and IFN- $\beta$  (21-24, 31-33). High and consistent levels of TNF- $\alpha$  down regulates proteins (e.g. nucleolin and isoform A of heterogeneous ribonucleoprotein) that bind to the  $\alpha$  and  $\beta$  motifs of the transcriptional initiator element of the CD28 gene, which prevent transcription of this gene (22, 24, 31). This suggests that a chronic pro-inflammatory environment can cause the origination of the CD4+CD28null T cell subset.

Another factor considered to be causative for CD28 loss is chronic antigen stimulation, and in specific chronic stimulation by cytomegalovirus (CMV) infection (22, 23, 29, 34, 35), suggesting that CD4+CD28null T cells are a subset of memory T cells. CMV belongs to the family of herpesviruses and in particular the betaherpesviruses, which are latent viruses. This implies that once a human is infected with the virus, it persists throughout life (23) and could stimulate the immune system occasionally and thus chronically stimulate T cells. Hence CMV may play a role in the origin of CD4+CD28null T cells.

Research has shown that the presence of a CMV infection increases the number of CD4+CD28null T cells (22, 29, 34, 35). Preliminary data of our own research group confirms this (figure 2). Figure 2 shows the percentage of CD4+CD28null T cells in MS patients that are seropositive or seronegative for CMV. The percentages of CD4+CD28null T cells are significantly higher in MS patients that are seropositive for CMV compared with MS patients that are seronegative for CMV infection.

Figure 2 also suggests that not every MS patient has an expansion of CD4+CD28null T cells, leading us to believe that a different disease course of MS between patients with low versus high numbers of CD4+CD28null T cells may be possible (19). Since a difference in the expansion of the CD4+CD28null T cells is seen between MS patients, a genetic predisposition for this expansion could be present. Research has shown that certain single nucleotide polymorphisms (SNPs) in the MHC class I polypeptide-related sequence B (MicB, rs2523651) and toll-like receptor 2 (TLR-2, rs5743708) genes are associated with an increased risk of CMV infection (36-38). The MicB gene encodes for a ligand for NKG2D, which is a receptor on natural killer cells, CD8+ T cells and the CD4+CD28null T cell subset. Binding of MicB to NKG2D causes the activation of a cytolytic response. The rs2523651 SNP in this gene possibly prevents the interaction of MicB and its receptor, leading to a reduced cytolytic response. The TLR-2 gene encodes for the TLR-2 receptor, which is a receptor on immune cells. The rs5743708 SNP in this gene probably leads to a functional defect in the receptor, resulting in a prohibited cytolytic response.

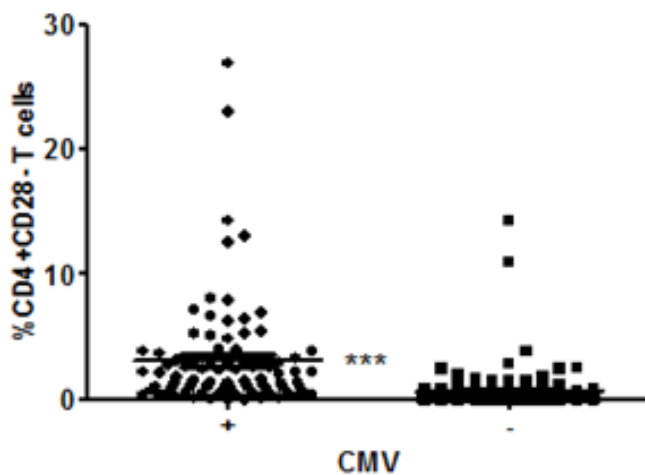


**Figure 2: Percentage of CD4+CD28null T cells in CMV seropositive and CMV seronegative MS patients.**

Blood samples of MS patients seropositive (+) and seronegative (-) for CMV (n= 212) were analyzed for the percentage of CD4+CD28null T cells. \*\*\*:  $p < 0.0001$  (Mann-Whitney test)

As was mentioned above CMV seropositivity may play a role in the expansion of the CD4+CD28null T cells, thus people having SNPs in the MicB and TLR-2 genes may have an increased risk of expanded CD4+CD28null T cells.

#### 5.4 Aim of this study

As mentioned in section 5.2 CD4+CD28null T cells have many characteristic that make them able to contribute to the pathology of MS. However, the way they originate and the precise role they play in MS is still unknown. That is why in this study the role and the origin of the CD4+CD28null T cell subset in the pathogenesis of MS will be studied. Our research group hypothesizes that CD4+CD28null T cells induce an immune response towards auto-antigens and originates due to chronic stimulation by CMV.

To investigate the role of these cells in MS, multiple experiments will be performed. First of all, their reaction towards several auto-antigens (myelin basic protein (MBP), myelin oligodendrocyte

glycoprotein (MOG)) will be tested. Second of all, the differentiation that they induce in other cells will be investigated. And last of all, their reaction towards MS relevant cells, such as oligodendrocytes and astrocytes, will be determined.

To investigate the origin of the CD4+CD28null T cells several experiments will be conducted. First, the proliferation of the CD4+CD28null T cells towards exposure to chronic stimulation by a CMV derived protein (pp65) will be measured. Secondly, the SNPs discussed above will be measured in MS patients to determine the risk for CD4+CD28null T cell expansion.

Next to determining the role and origin of the CD4+CD28null T cells, the presence of these cells in an experimental autoimmune encephalomyelitis (EAE) mouse model will be investigated. EAE is an animal model of brain inflammation and is widely used as animal model of MS. To our knowledge the presence of the CD4+CD28null T cell subset in an EAE mouse model has not been investigated before. Blood samples will be taken and organs (brain, lymph nodes, spleen, spinal cord) will be isolated to determine if the CD4+CD28null T cells are present. Slides of the brain and spinal cord will be taken. The slides will be immunohistochemically stained to be able to tell where the CD4+CD28null T cells are located if present in these organs. The presence of CD4+CD28null T cells in the EAE mouse model could give us more insight in the *in vivo* properties of these cells, and could lead to validation of the *in vitro* findings.

## 6 Materials and methods

### 6.1 Identification of CD4+CD28null T cells by means of flow cytometry

The CD4+CD28null T cell fraction in the peripheral blood of all donors was determined. Peripheral blood mononuclear cells (PBMCs) were isolated from whole blood by density gradient centrifugation. Briefly, blood samples were centrifuged at 2000 rpm for 10 minutes. After which the plasma was removed. Next, phosphate buffered saline (PBS) (Lonza, Basel, Switzerland) containing 2mM of ethylenediaminetetraacetic acid (EDTA) (Ambion, Carlsbad, CA, USA) was added to dilute the blood. The blood was transferred on top of a ficoll (Cedarlane, Burlington, Ontario, Canada) layer, and was centrifuged at 1800 rpm for 20 minutes. Next, PBMCs were isolated and washed and could be used for flow cytometric analysis.

CD4+CD28null T cells were differentiated from the whole blood cell population by staining the cells with anti-human CD4 PerCP (BD Biosciences, Franklin Lakes, NJ, USA) and CD28 APC (BD Pharmingen, San Diego, CA, USA). Further phenotyping of the CD4+CD28null T cell population was done by using the following antibodies: anti-human CD45RO PE Texas Red CF 594 (BD Biosciences, Franklin Lakes, NJ, USA), CD45RA APC H7 (BD Pharmingen).

Cells were analyzed by flow cytometry using FACSaria II (BD Biosciences).

### 6.2 CMV assay

PBMCs were isolated from peripheral blood of three donors (see table 1; this experiment was performed twice) by density gradient centrifugation. The donors were chosen for their different characteristics in CMV serology, and CD4+CD28null T cell expansion. PBMCs of each donor were plated out in a 96 well plate at a concentration of 250.000 cells per well in culture medium (RPMI-1640 (Lonza) with 10% heat inactivated fetal bovine serum (FBS), 1% non-essential amino acids, 0,5% penicillin streptomycin, 1% sodiumpyruvate). Eight time points (day 0, day 1, day 6, day 9, day 12, day 15, and day 20) were chosen for each donor to measure the percentage of CD4+CD28null T cells. Three conditions per donor were used. Namely, a condition in which IL-2 (50U per ml) (Roche, Penzberg, Germany) or CMV pp65 (10µg per ml) (MACS, Miltenyi Biotec, Bergisch Gladbach, Germany) is supplemented, and a condition in which both are added. CMV pp65 was supplemented on day 0, and restimulations were done every week with CMV pp65 pulsed in autologous PBMCs (100.000 cells per well) that were irradiated (82,75 Gy). IL-2 was supplemented every 2-3 days. The percentage of CD4+CD28null T cells was measured by flow cytometry as mentioned in section 6.1.

**Table 1: Characteristics of the donors used in the CMV assay.**

Donor 1, 2 and 3 were donors used in the first CMV assay. Donor 4, 5, and 6 were donors used in the second CMV assay.

| Donor ID       | CMV seropositive | CD4+CD28null T cell expansion |
|----------------|------------------|-------------------------------|
| <b>Donor 1</b> | Yes              | No                            |
| <b>Donor 2</b> | No               | No                            |
| <b>Donor 3</b> | Yes              | Yes                           |
| <b>Donor 4</b> | No               | No                            |
| <b>Donor 5</b> | Yes              | Yes                           |
| <b>Donor 6</b> | Yes              | No                            |

### **6.3 Stimulation of MBP specific T cell clones with MBP and PHA**

MBP specific T cell clones were cultured in a 96 well plate at a concentration of 250.000 cells per well in culture medium. Every week the T cell clones were stimulated with MBP (100µg/ml) and PHA (2µg/ml) pulsed in autologous PBMCs (100.000 cells per well) that were irradiated (82,75 Gy). The percentage of CD4+CD28null T cells was measured by flow cytometry as mentioned in section 6.1.

### **6.4 Optimization of the differentiation assay**

#### **6.4.1 Standard polymerase chain reaction**

The functionality of the primers (see table 2) of the differentiation assay was tested. This was done by performing a standard polymerase chain reaction (PCR).

The PCR mix contained 20mM dNTP's, 10µM reverse primer, 10µM forward primer, 10x PCR reaction buffer, 5U/µl Taq polymerase, and a varying amount of mQ per sample (total volume 9µl). 10µl of cDNA was added to the PCR mix.

The samples were then subjected to the following PCR program in the iCycler Thermal Cycler (Bio-Rad, California, USA): first an initial denaturation of 5 minutes at 95°C; followed by 40 cycles of denaturation of 20 seconds at 95°C, annealing of 20 seconds at 60°C, and elongation of 40 seconds at 72°C; next a final elongation of 7 minutes at 72°C; lastly the samples were hold at 4°C.

Next the PCR products were loaded on a 2% agarose gel together with a 25bp and 100bp ladder (Invitrogen, Carlsbad, CA, USA) to check length of the amplified products.

#### **6.4.2 Sequencing PCR**

A second optimization step included a sequencing PCR of the amplified PCR products of the standard PCR.

The PCR mix contained Big Dye Terminator v1.1 5x sequencing buffer (Applied Biosystems, Foster City, CA, USA), Big Dye Terminator v1.1 cycle sequencing RR-100 (Applied Biosystems), 2µM primer (forward or reverse), and a varying amount of mQ per sample. 1µl of PCR product from a standard PCR was added to the mix. Samples underwent the following PCR program: hot start (90°C); 30 seconds at 96°C; 25 cycles of 10 seconds at 96°C, 5 seconds at 50°C, and 4 minutes at 60°C; samples were hold at 4°C.

The PCR products from the sequencing PCR were then purified by means of sephadex G-50 (GE Healthcare). First sephadex columns were made. Next the PCR products were pipetted onto the sephadex columns. The columns were centrifuged for 2 minutes at 3200rpm, which resulted in a purified PCR product. Then the PCR products were evaporated in the concentrator plus (Eppendorf, Hamburg, Germany). After evaporation the PCR products were resolved in 25µl HiDi Formamide (Applied Biosystems) and transferred to sequence eppendorfs. Samples were then sequenced with the ABI Prism 310 Genetic Analyzer (Applied biosystems).

#### **6.4.3 Differentiation assay using cytokine cocktail**

After determining the functionality of the primers, a test was performed to see if the differentiation assay worked. In this test cytokines instead of CD4+CD28null T cell supernatant were used to cause differentiation.

PBMCs were isolated from blood by density gradient centrifugation. CD14+ cells (monocytes) were isolated from PBMCs by using the EasySep positive selection human CD14 selection kit according to the manufacturer's protocol (Stemcell Technologies, Vancouver, British Columbia, Canada). The CD14+ cells were plated out in a 6 well plate at a concentration of 600.000 cells per well in culture medium. The CD14- portion of the positive selection was subjected to a negative selection to acquire CD4+CD45RO+ T cells (memory CD4+ T cells), by using the CD4+ memory T cell isolation kit according to the manufacturer's protocol (MACS, Miltenyi Biotec). The CD4+CD45RO+ T cells were co-cultured with the CD14+ cells at a concentration of 1.000.000 cells per well. Anti-CD3 (1 mg/ml) was added to stimulate the cells.

**Table 2: The primers used in the differentiation assay.**

Names of the primers, their sequence, number of bases, melting temperature, percentage of guanine and cytosine (GC) nucleotides and amplicon length according to BLAST search are given. GATA-3 and IL-4 primers were used to measure Th2 differentiation. ROR $\gamma$ T and IL-17 primers were used for measuring Th17 differentiation. T-bet and IFN $\gamma$  primers were used to measure Th1 differentiation.

| Name Primer            | Sequence                        | bp | Tm | % GC nucleotides | Amplicon length (bp) |
|------------------------|---------------------------------|----|----|------------------|----------------------|
| GATA-3 forward         | AGG-CCC-GGT-CCA-GCA-CAG-AA      | 20 | 66 | 65               | 174                  |
| GATA-3 reverse         | TGG-CTG-CAG-ACA-GCC-TTC-GC      | 20 | 66 | 65               |                      |
| IL-4 forward           | ACA-GCC-TCA-CAG-AGC-AGA-AGA-CTC | 24 | 54 | 54.2             | 121                  |
| IL-4 reverse           | AAC-TGC-CGG-AGC-ACA-GTC-GC      | 20 | 66 | 65               |                      |
| ROR $\gamma$ T forward | CTG-GAC-CAC-CCC-CTG-CTG-AGA     | 21 | 55 | 66.7             | 163                  |
| ROR $\gamma$ T reverse | GGA-AGA-AGC-CCT-TGC-ACC-CCT-CA  | 23 | 56 | 60.9             |                      |
| IL-17 forward          | ATG-GCC-CAG-CCA-TGG-TCA-AGT-A   | 22 | 52 | 54.5             | 132                  |
| IL-17 reverse          | GCA-CAG-GCG-GGC-AAC-TCT-CA      | 20 | 66 | 65               |                      |
| T-bet forward          | GAG-GAC-TAC-GCG-CTA-CCC-GC      | 20 | 68 | 70               | 138                  |
| T-bet reverse          | TGG-GAA-CAT-CCG-CCG-TCC-CT      | 20 | 66 | 65               |                      |
| IFN $\gamma$ forward   | GGG-GCC-AAC-TAG-GCA-GCC-AAC     | 21 | 55 | 66.7             | 145                  |
| IFN $\gamma$ reverse   | AAG-CAC-TGG-CTC-AGA-TTG-CAG-GC  | 23 | 54 | 56.5             |                      |

GATA-3: Trans-acting T-cell-specific transcription factor; IL-4: Interleukin-4; ROR $\gamma$ T: RAR-related orphan receptor gamma T; IL-17: Interleukin-17; T-bet: T-box transcription factor TBX21; IFN $\gamma$ : Interferon gamma; bp: basepairs.

Th1 cell differentiation was performed by adding human anti-IL-4 (5 µg/ml) and IL-12 (10 ng/ml) (R&D systems, Minneapolis, MN, USA). Th2 cell differentiation was achieved by administering human anti-IFN-γ (5 µg/ml), IL-4 (200 ng/ml) (R&D systems), and anti-IL-12 (5 µg/ml) (eBioscience). Lastly, Th17 differentiation was performed by adding human anti-IL-4 (5 µg/ml), anti-IFN-γ (5 µg/ml), and IL-23 (25 ng/ml) (R&D systems).

The co-culture lasted for 6 days, after which the cells were analyzed by using real time PCR. Before real time PCR analysis, pellets of the co-culture were made by centrifuging cells at 13000 rpm for 30 seconds.

#### **6.4.3.1 Determining gene expression**

Pellets of the co-cultures were subjected to RNA isolation, which was accomplished by using the RNeasy Mini Kit according to the manufacturer's protocol (Qiagen, Hilden, Germany). The RNA from the samples was then transcribed to cDNA by using qScript cDNA supermix according to manufacturer's protocol (Quanta BioSciences, Gaithersburg, USA). cDNA from the samples was then used for real time PCR (qPCR) analysis. The qPCR mix contained SYBR green, 10µM forward primer, 10µM reverse primer, and a varying amount of nuclease free water (total volume of 7.5µl). 2.5µl of cDNA (5ng/µl) was added to the mix and samples were subjected to the following PCR program: 20 seconds at 95°C; 40 cycles of 3 seconds at 95°C and 30 seconds at 60°C; a melting curve stage of 15 seconds at 95°C, 1 minute at 60°C, and 15 seconds at 95°C. Samples were processed with the StepOnePlus real time PCR system (Applied Biosystems) and results were analyzed with StepOne Software v2.2.2 (Applied Biosystems) and qBase (Biogazelle, Zwijnaarde, Belgium). Samples were normalized against the best fitted housekeeping genes (YWHAZ, CycA, HMBS, and ActB), as determined by geNorm (Ghent University, Belgium).

Melt curves of the primers (table 2) were obtained after qPCR analysis, which were used to look at possible non-specific amplification.

## **6.5 EAE mouse model**

### **6.5.1 Immunization**

C57BL/6J0laHsd (Harlan Laboratories, Indianapolis, Indiana, USA) female mice (n=25) at the age of 10 weeks were used in the EAE model. Animals were weighed and scored (see table 2s) daily. Immunization and scoring of the mice was done according to the manufacturer's protocol (EAE induction by active immunization in C57BL/6 mice, Hooke Laboratories, Lawrence, KS, USA).

Briefly, 8 weeks old mice were able to acclimatize 14 days before EAE induction. EAE immunization was performed by injecting pertussis toxin (PTX) and an emulsion of MOG<sub>35-55</sub> in complete Freund's adjuvant (CFA). At day 0 the MOG<sub>35-55</sub>/CFA emulsion (0.1mL) was administered subcutaneously in the upper and lower back of the mice. Moments after the MOG<sub>35-55</sub>/CFA emulsion injection the first PTX solution (0.1mL) was administered intraperitoneally. After 24 hours the second PTX injection (0.1mL) was performed. 9-14 days after induction EAE symptoms became apparent.

The mice were divided into 5 groups (each group consisted of 5 mice); 2 control groups that were sacrificed after 90 days, in which both groups received a CFA injection (without MOG<sub>35-55</sub>) and one control group received the PTX injections; 3 EAE groups, in which one group was sacrificed after 30 days, one group after 60 days and the last group after 90 days.

Mice were sacrificed 30, 60, and 90 days after EAE induction and lymph nodes, brain, spinal cord and spleen were isolated. Lymph nodes, spleen, sections of brain and spinal cord were stored in PBS, after which the cells were isolated (see section 6.5.2) for flow cytometry analysis (see section 6.5.3). The other sections of the brain and spinal cord were stored in 4% paraformaldehyde (PFA) at 4°C. After 24 hours the 4% PFA solution was substituted with a 4% PFA 5% sucrose solution, which was again substituted with a 4% PFA 30% sucrose solution after 24 hours. Next, these brain and spinal cord sections were frozen by means of liquid nitrogen. First brain and spinal cord sections were placed in a mold filled with tissue tek. The molds were placed in isopentane and were frozen at -50°C, after which they were put in liquid nitrogen for a short duration. Next, these organ sections were stored at -80°C. Organs were stained immunohistochemically (see section 6.5.4) to check for the presence of CD4+CD28null T cells.

## **6.5.2 Isolation of cells**

After sacrificing the mice at day 30, day 60, and day 90 after EAE immunization, lymph nodes, spleen and spinal cord and brain sections were isolated and stored in PBS at 4°C before usage.

### **6.5.2.1 Blood**

Blood from 3 mice from each group was drawn retro-orbitally at several time points (day -4, day 3, day 10, day 17, day 31, day 45) before or after EAE induction (day 0) to measure the amount of CD4+CD28null T cells by flow cytometry (see section 6.5.3).

### **6.5.2.2 Brain and spinal cord**

The brain and spinal cord sections were cut down in small pieces and transferred to a 13.7% collagenase type 1A/culture medium mixture (collagenase type 1A (Sigma Aldrich, Seelze, Germany) (125 collagen digestion units)). After incubation for 1 hour at 37°C, the organ pieces were triturated with culture medium. Next, PBS was added and the organ pieces were triturated for a second time. Samples were centrifuged at 300g and 4°C for 5 minutes. Pellets were resuspended in 30% percoll (GE Healthcare, Little Chalfont, Buckinghamshire, UK) and centrifuged at 700g for 10 minutes. Fatty tissue and supernatant were removed and pellets were resuspended with PBS. Samples were transferred on a cell strainer to remove impurities. Next, the samples were centrifuged at 1800rpm and 4°C for 5 minutes. Cells were dissolved in culture medium, counted and used for flow cytometric analysis (see section 6.5.3).

### **6.5.2.3 Spleen**

Spleens were transferred to a cell strainer and grinded to get a cell solution. Samples were centrifuged at 1400rpm for 10 minutes and pellets were dissolved in PBS. The white blood cells from these solutions were isolated by density gradient centrifugation using ficoll Histopaque-1077 (Sigma Aldrich, Seelze, Germany). PBMCs were dissolved in culture medium, counted and used for flow cytometric analysis (see section 6.5.3).

### **6.5.2.4 Lymph node**

Lymph nodes were transferred to a cell strainer and mashed to get a cell suspension. Next lymph nodes were centrifuged at 1400rpm for 10 minutes. Pellets were dissolved in culture medium, counted and used for flow cytometric analysis (see section 6.5.3).

### **6.5.3 Identification of CD4+CD28null T cells**

The CD4+CD28null T cell fraction in the peripheral blood and organs of mice for the EAE mouse model was determined. Cells were stained with anti-mouse CD4 PerCP-Cy5.5 and CD28 APC (eBioscience, San Diego, CA, USA) to differentiate CD4+CD28null T cells from the rest of the cell population. The CD4+CD28null T cells were further phenotyped by using the following antibodies: anti-mouse CD62L FITC, CD27 PE, CD3 Efluor 780 APC, NKG2D PE Cy7, granzyme B FITC (eBioscience), CD127 PE CF 594, and IFN- $\gamma$  PE CF 594 (BD Biosciences). Cells were analyzed by flow cytometry using FACSaria II (BD Biosciences).

### **6.5.4 Immunohistochemistry**

Slices (10 $\mu$ m) of brain and spinal cord of the C57BL/6 female mice were made by using the Leica CM3050S cryostat (Leica Biosystems, Nussloch, Germany). The microscopic slides were stored at -20°C prior to use.

#### **6.5.4.1 Fluorescent staining**

The slides were thawed 30 minutes before staining. A Dako pen (Dako, Glostrup, Denmark) was used to apply a barrier around the tissue of the brain and spinal cord. The tissues were washed and shaken 3 times for 5 minutes each time in PBS (washing step). NH<sub>4</sub>Cl was added to the slides to reduce background signal, slides were incubated for 30 minutes at room temperature (RT). Spinal cord slides were blocked with 10% serum (depending on the secondary antibody) in PBS at RT for 30 minutes. After blocking the rat anti-mouse CD3, rabbit anti-mouse CX<sub>3</sub>CR1, or rat anti-mouse CD4 (1/100 in PBS) was added. Slides were incubated overnight at 4°C, after which the slides were washed, to remove the primary antibody. Next, the slides were incubated with goat anti-rat alexa fluor 555 (for CD3), donkey anti-rabbit alexa fluor 555 (for CX<sub>3</sub>CR1), or goat anti-rat alexa fluor 555 (for CD4) (1/800 in PBS) for one hour at RT. After washing, the spinal cord slides were incubated with 4',6-diamidino-2-phenylindole (DAPI) for 10 minutes, in order to stain the nuclei. The slides were washed, after which they were incubated with Sudan Black (0.1% in 70% Ethanol) to reduce background signal. Next, the slides were first washed in 70% ethanol and subsequently in PBS. The slides were washed and shaken for 5 minutes in milli-Q (mQ). Fluorescent aqueous mounting medium (Dako) was added after which the cover was placed. Images of the slides were taken with the Nikon Eclipse 80i fluorescent microscope (Nikon, Shinjuku, Tokyo, Japan) and NIS elements viewer (Nikon).

## **6.6 Statistics**

Statistics were performed by using GraphPad Prism version 5.01. Two-way ANOVA analysis was performed on the CMV assay data, the data from the EAE model when comparing the control groups with the EAE group.

Linear regression analysis was used to measure a positive correlation between CD4+CD28null T cell percentage compared to an increase in EAE score.

## 7 Results

The aim of our study was to determine several characteristics of the CD4+CD28null T cell subset. This was accomplished by performing CMV assays to determine the origin of the CD4+CD28null T cells, a differentiation assay to know what kind of differentiation these cells induce, and an EAE pilot study to determine several *in vivo* characteristics of the CD4+CD28null T cells.

### 7.1 Percentage of CD4+CD28null T cell expansion in MS and HC donors

To create a broader view with regard to the presence of the CD4+CD28null T cell subset in the general population, their percentage in the peripheral blood of MS and HC donors was determined (figure 3). A cut off value of 2% determined if there was an expansion.

12 out of the 43 MS donors showed an expansion of the CD4+CD28null T cells, meaning that 27.9% of MS patients have an expansion of this cell subset.

When looking at the HC donors, 10 out of 53 donors show an expansion, meaning that 18.9% of HC have an expansion of these cells.

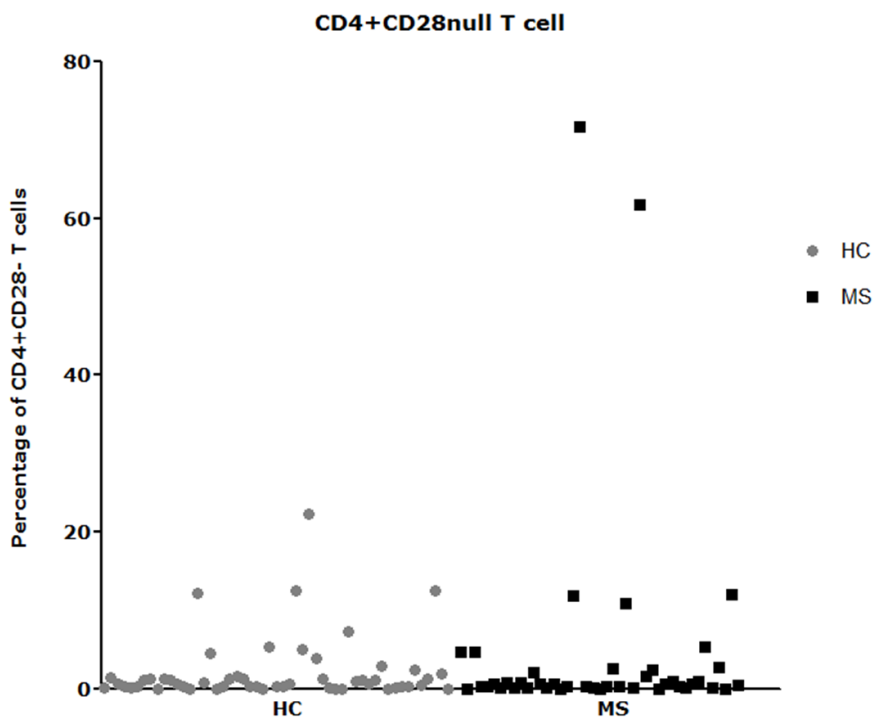


**Figure 3: The percentage of CD4+CD28null T cells in peripheral blood from HC and MS donors.** PBMCs were isolated from peripheral blood of HC (n=53) and MS (n=43) donors. PBMCs were stained with CD4 and CD28 labels to determine CD4+CD28null T cell percentage by means of flow cytometry. HC: healthy control; MS: multiple sclerosis patient; PBMC: peripheral blood mononuclear cell.

### 7.2 *In vitro* stimulation of MBP specific T cell clones with MBP and PHA

To determine if the CD4+CD28null T cells had autoreactive properties, an *in vitro* experiment with MBP and PHA stimulation was conducted. In this experiment MBP specific T cell clones were stimulated with MBP and PHA (figure 4).

When looking at figure 4, an increasing trend in the percentage of CD4+CD28null T cells within the T cell clones was observable after several rounds of stimulation.

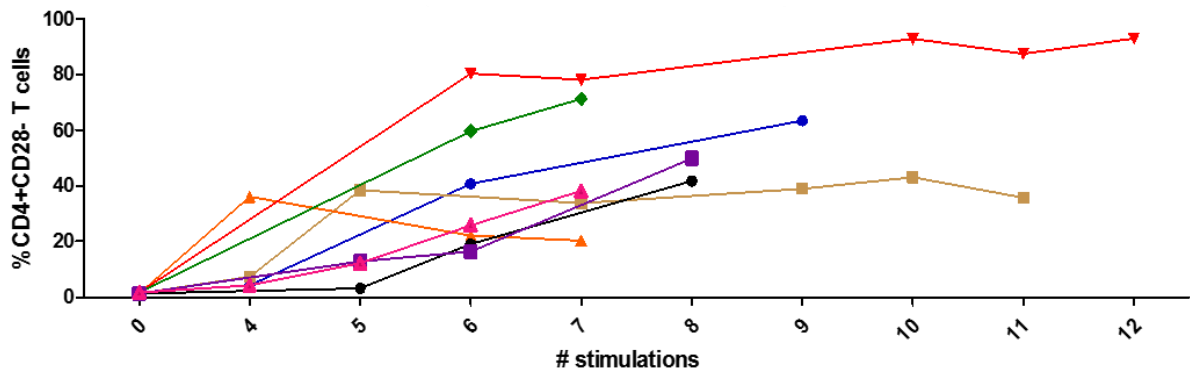


**Figure 4: The percentage of CD4+CD28null T cells within the MBP specific T cell clones after stimulation with MPB and PHA.**

### 7.3 *In vitro* proliferation of CD4+CD28null T cells by means of CMV assays

Our research group hypothesized that CD4+CD28null T cells would originate due to chronic CMV stimulation. To see if this was the case, PBMCs from different donors were cultured for 30 days and subjected to IL-2, CMV, or IL-2 + CMV stimulation (figure 5 A-C). After every time point PBMCs were analyzed by flow cytometry to measure the CD4+CD28null T cell percentage. Two CMV assays were performed, each with different donors (see section 6.2, table 1).

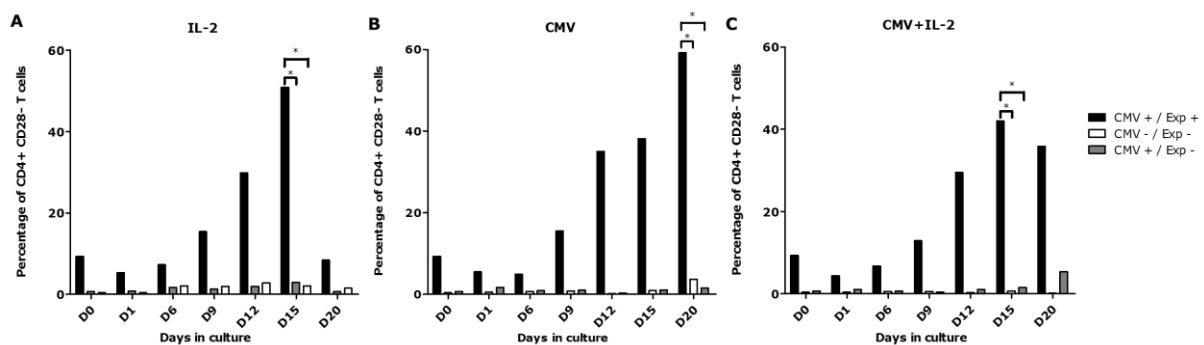


**Figure 5: The percentage of CD4+CD28null T cells at different time points subjected to a stimulatory environment.** PBMCs from 3 donors were cultured for a maximum of 20 days in (A) an IL-2, (B) a CMV, (C) an IL-2 and CMV stimulatory condition. After D0, D1, D6, D9, D12, D15, D20, and D30 PBMCs were stained with CD4 and CD28 labels. The percentage of CD4+CD28null T cells was measured by means of flow cytometry. Two way ANOVA was performed to find statistical differences in the cell percentage between groups (\*:  $P < 0.05$ ). PBMC: peripheral blood mononuclear cell; IL-2: interleukin-2; CMV: cytomegalovirus; CMV+Exp+: cytomegalovirus seropositive donor with CD4+CD28null T cell expansion; CMV+Exp-: cytomegalovirus seropositive donor without CD4+CD28null T cell expansion; CMV-Exp-: cytomegalovirus seronegative donor without CD4+CD28null T cell expansion.

Figure 5 A shows the percentage of the CD4+CD28null T cell subset in a condition in which only IL-2 is supplemented. A rising trend in the percentage of the CD4+CD28null T cell subset is seen in CMV seropositive donor with CD4+CD28null T cell expansion (CMV+/Exp+) after several days in culture. At day 20 and 30 of the experiment a decreasing trend in the percentage of CD4+CD28null T cells in the CMV+/Exp+ donor is seen. No response in the percentage of the CD4+CD28null T cells of the other donors is noticeable. A significant difference in the number of CD4+CD28null T cells can

be observed between the CMV+/Exp+ and the CMV+/Exp- donor, and the CMV+/Exp+ and the CMV-/Exp- donor at day 15 ( $P < 0.05$ ).

When looking at the percentage of CD4+CD28null T cells of the CMV+/Exp+ donor in a CMV stimulatory environment, a rising trend can be observed after D6 (figure 5 B). For the CMV+/Exp- and CMV-/Exp- donor no rising or diminishing trend of the percentage of CD4+CD28null T cells in the CMV stimulatory environment can be seen. At day 20 the percentage of CD4+CD28null T cells significantly differ between the CMV+/Exp+ and CMV+/Exp- donor, and the CMV+/Exp+ and CMV-/Exp- donor ( $P < 0.05$ ).

Figure 5 C shows the percentage of CD4+CD28null T cells of the CMV+/Exp+, CMV+/Exp-, and CMV-/Exp- donors in a CMV+IL-2 stimulatory environment. An increasing trend in the percentage of the CD4+CD28null T cell subset is observable for the CMV+/Exp+ donor after D1. No elevating trend in the percentage of CD4+CD28null T cells is observed for the other donors. The percentage of CD4+CD28null T cells show a significant difference at day 15 between the CMV+/Exp+ and CMV+/Exp- donor, and the CMV+/Exp+ and CMV-/Exp- donor ( $P < 0.05$ ).

The CMV assay was performed for a second time (figure 6), but with other donors were used (see table 1). Figure 6 shows the percentage of CD4+CD28null T cells from 3 donors at several time points subjected to a certain condition.

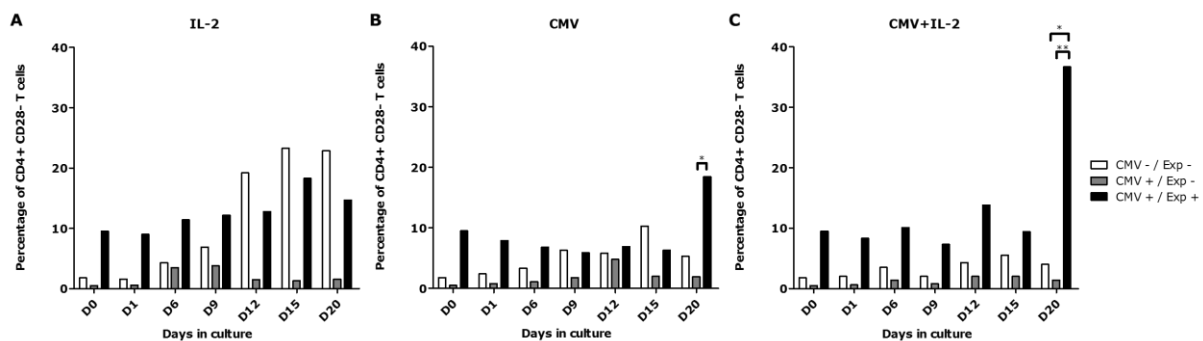


**Figure 6: The percentage of CD4+CD28null T cells from 3 donors at different time points in a stimulatory condition.**

PBMCs from 3 donors were cultured for a maximum of 20 days in which (A) IL-2 was supplemented, (B) CMV was added, (C) both IL-2 and CMV were supplemented. After each time point PBMCs were stained with CD4 and CD28 labels and analyzed by means of flow cytometry to determine the frequency of CD4+CD28null T cell. Two way ANOVA was performed to find statistical differences in the cell percentage between groups (\*:  $P < 0.05$ ; \*\*:  $P < 0.01$ ). PBMC: peripheral blood mononuclear cell; IL-2: interleukin-2; CMV: cytomegalovirus; CMV+Exp+: cytomegalovirus seropositive donor with CD4+CD28null T cell expansion; CMV+Exp-: cytomegalovirus seropositive donor without CD4+CD28null T cell expansion; CMV-Exp-: cytomegalovirus seronegative donor without CD4+CD28null T cell expansion.

When looking at figure 6 A, a trend of increasing CD4+CD28null T cells starting from D0 from the CMV+/Exp+ and CMV-/Exp- donors in a IL-2 stimulatory condition can be observed. No trend of increasing CD4+CD28null T cells is seen in the CMV+/Exp- donor. No significant differences in the number of CD4+CD28null T cells between donors can be found.

Figure 6 B shows the percentage of the CD4+CD28null T cell subset in a CMV stimulatory condition. An increasing trend of the CD4+CD28null T cells starting from D0 until D15 from the CMV-/Exp- can be noticed. The CMV+/Exp+ donor shows a decreasing trend in the number of CD4+CD28null T cells starting from D0 until D9, after which an increasing trend can be noticed from D15. No effect is seen in the percentage of CD4+CD28null T cells from the CMV+/Exp- donor. A significant difference at

day 20 in the number of CD4+CD28null T cells can be observed between the CMV+/Exp- and CMV+/Exp+ donor ( $P < 0.05$ ).

In figure 6 C the frequency of the CD4+CD28null T cells from 3 donors at different time points in a CMV and IL-2 stimulatory condition is shown. No trend in the percentage of CD4+CD28null T cells of the CMV+/Exp+ donor can be noticed. The CD4+CD28null T cells from the CMV-/Exp- show an increasing trend. The percentage of CD4+CD28null T cells from the CMV+/Exp- does not vary. A significant difference at D20 in the number of CD4+CD28null T cells can be noted between the CMV+/Exp+ and CMV-/Exp- donor ( $P < 0.05$ ), and the CMV+/Exp+ and CMV+/Exp- donor ( $P < 0.01$ ).

Figure 7 shows the results of three CMV assays combined (CMV assays from this study and a preliminary CMV assay), the percentage of CD4+CD28null T cells from 9 donors (3 CMV+Exp+, 3 CMV+Exp-, 3 CMV-Exp- donors) at several time points in a stimulatory environment can be observed. In figure 7 A an increasing trend in the percentage of CD4+CD28null T cells from the CMV+Exp+ donor in a CMV stimulatory environment can be noticed. No response from the other donors can be seen. A significant difference in the number of CD4+CD28null T cells at day 15 and day 20 between the CMV+Exp+ and CMV+Exp- donor, and the CMV+Exp+ and CMV-Exp- donor can be seen ( $P < 0.05$  at day 15,  $P < 0.01$  at day 20).

An upward trend in the CD4+CD28null T cell percentage from the CMV+Exp+ and CMV+Exp- donors in the CMV+IL-2 stimulatory environment can be observed (figure 7 B). No response of the CMV-Exp- donors can be noted. The percentage of CD4+CD28null T cells significantly differ at day 12 ( $P < 0.05$  between CMV+Exp+ and CMV+Exp- donors,  $P < 0.01$  between CMV+Exp+ and CMV-Exp- donors), day 15 ( $P < 0.01$  between CMV+Exp+ and CMV+Exp- donors, and  $P < 0.0001$  between CMV+Exp+ and CMV-Exp- donors) and day 20 ( $P < 0.0001$ ) between the CMV+Exp+ and CMV+Exp-, and CMV+Exp+ and CMV-Exp- donors.

In figure 7 C an increasing trend in the frequency of CD4+CD28null T cells from all donors in an IL-2 stimulatory environment can be noticed. At day 15 a significant difference between the CMV+Exp+ and CMV+Exp-, and CMV+Exp+ and CMV-Exp- donors can be found ( $P < 0.05$ ).

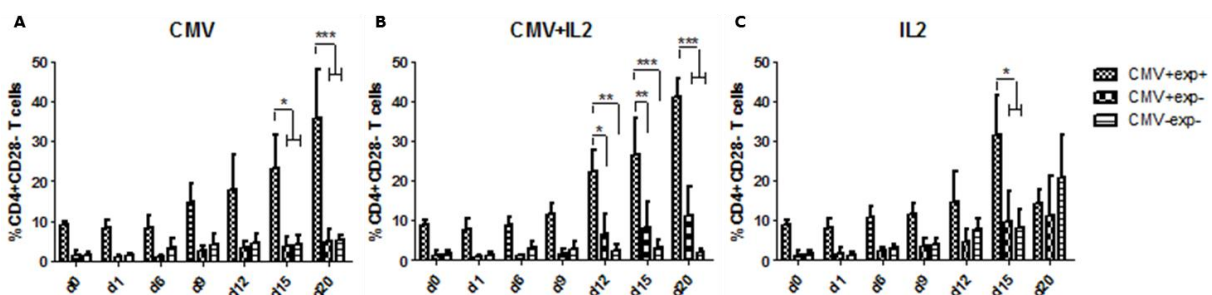


**Figure 7: Percentage of CD4+CD28null T cells at different time points in a stimulatory environment.** Results from three CMV assays were combined (3 CMV+Exp+, 3 CMV+Exp-, and 3 CMV-Exp- donors). Two way ANOVA was performed to find statistical differences in the cell percentage between groups (\*:  $P < 0.05$ ; \*\*:  $P < 0.01$ ; \*\*\*:  $P < 0.0001$ ). IL-2: interleukin-2; CMV: cytomegalovirus; CMV+Exp+: cytomegalovirus seropositive donor with CD4+CD28null T cell expansion; CMV+Exp-: cytomegalovirus seropositive donor without CD4+CD28null T cell expansion; CMV-Exp-: cytomegalovirus seronegative donor without CD4+CD28null T cell expansion.

Next to general CD4+CD28null T cell percentages, the amount of memory (CD45RO+) and naïve (CD45RA+) T cells within the CD4+CD28null T cell population was measured during the CMV assay. The percentage of CD45RO+CD45RA- cells within the CD4+CD28null T cell population stimulated with either IL-2, CMV, or CMV+IL-2 is shown in supplementary figure 1.

An upward trend in the percentage of the CD45RO+CD45RA- fraction of the general CD4+CD28null T cell population can be observed in every stimulatory condition and in each donor.

These data indicate that CD4+CD28null T cells are a memory T cell subset and that chronic stimulation of this cell subset leads to the development of a more memory T cell based population.

The percentage of naïve T cells within the CD4+CD28null T cell population stimulated with IL-2, CMV, or CMV+IL-2 can be observed in figure 8.

Figure 8 A shows the CD45RO-CD45RA+ T cells in an IL-2 stimulatory condition. The CD45RO-CD45RA+ T cell percentage shows a decreasing trend in the CMV+/Exp+ donor. In the CMV-/Exp- and CMV+/Exp- donor the CD45RO-CD45RA+ fraction shows a decrease at day 1, an increase at day 6, and a decreasing trend again until day 20. No significant differences between groups could be found.

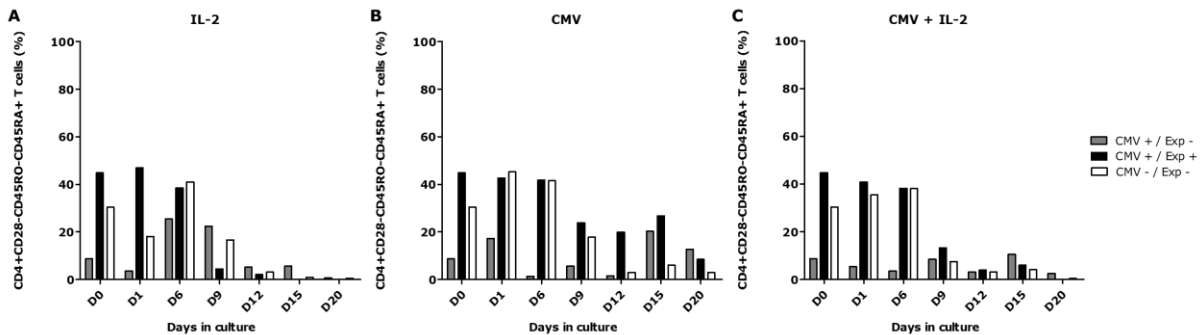


**Figure 8: The percentage of CD4+CD28null CD45RO-CD45RA+ T cells from 3 donors at several time points in a different stimulatory environment.** PBMCs from three donors with different characteristics (CMV+/Exp+, CMV+/Exp-, and CMV-/Exp-) were cultured for a maximum of 20 days in a condition in which (A) IL-2, (B) CMV, (C) CMV+IL-2 was added. Two way ANOVA was performed to find statistical differences in the cell percentage between groups. PBMC: peripheral blood mononuclear cell; IL-2: interleukin-2; CMV: cytomegalovirus; CMV+/Exp+: cytomegalovirus seropositive and CD4+CD28null T cell expansion positive donor; CMV+/Exp-: cytomegalovirus seropositive and CD4+CD28null T cell expansion negative donor; CMV-/Exp-: cytomegalovirus seronegative and CD4+CD28null T cell expansion negative donor.

In the CMV stimulatory condition (figure 8 B), the number of CD45RO-CD45RA+ T cells show a decreasing trend for the CMV+/Exp+ and CMV-/Exp- donors. While the CD45RO-CD45RA+ T cell percentage for the CMV+/Exp- donor shows an alternating pattern, which in the end does not vary from the starting percentage. No significant differences in the number of CD4+CD28null CD45RO-CD45RA+ T cells between the donors could be found.

In figure 8 C the number of CD45RO-CD45RA+ T cells can be observed. A downward trend for the CMV+/Exp+ and CMV-/Exp- donor can be noticed. The percentage of CD45RO-CD45RA+ T cells from the CMV+/Exp- donor shows an alternating pattern of slight decreases and increases, however at day 20 this cell percentage is at the same level as that of the other donors.

These data show that the CD4+CD28null T cells are not a naïve cell population and that chronic stimulation causes these cells to lose the CD45RA+ marker.

## 7.2 Differentiating capacities of CD4+CD28null T cells

Next to the origin of the CD4+CD28null T cells, our research group wanted to further characterize this cell subset with regard to the differentiation they could induce. This could be accomplished by performing a differentiation assay. However, first this assay had to be optimized.

### 7.2.1 Functionality of primers

Optimization of the differentiation assay included testing the primers for their functionality. Figure 9 shows a 2% agarose gel which was loaded with the PCR samples from three different donors (donor A, B, and C). These PCR samples were amplified with the primers listed in table 2. All loaded PCR products showed bands with the expected length (the correct length of the amplicons was acquired by alignment of the primers with the corresponding sequence on BLAST; see table 2).

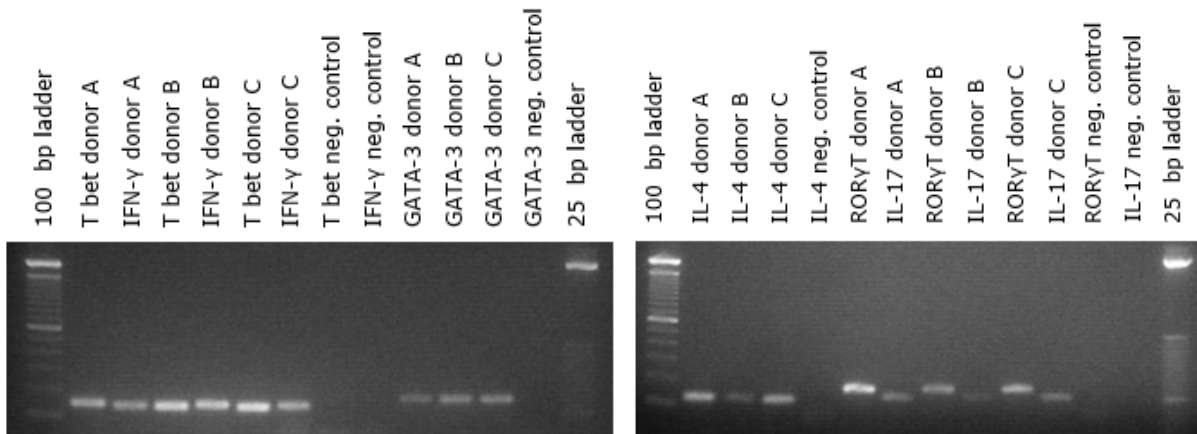


**Figure 9: A 2% agarose gel containing the PCR products of different donors (donor A, B, and C).** Bands with the expected length (see table 2) can be observed in all samples. GATA-3: Trans-acting T-cell-specific transcription factor; IL-4: Interleukin-4; ROR $\gamma$ T: RAR-related orphan receptor gamma T; IL-17: Interleukin-17; T-bet: T-box transcription factor TBX21; IFN- $\gamma$ : Interferon gamma.

Next to a 2% agarose gel containing the PCR samples, a sequencing of the primers with cDNA samples was performed. This was done to check if the primers amplified the correct cDNA fragments. Figure 10 shows the sequencing result when T-bet reverse primer was used. The displayed sequence was used in a BLAST search to check if the correct sequence was amplified (table 3).

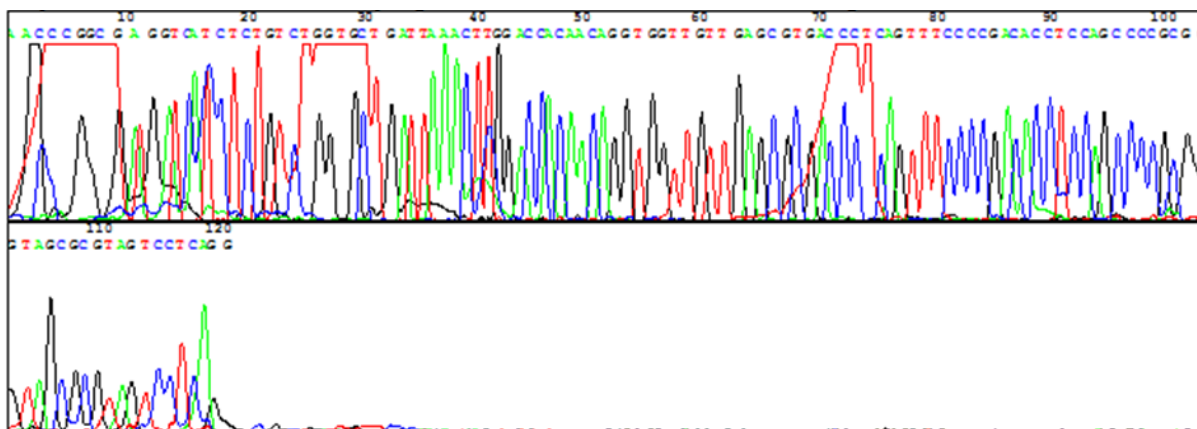


**Figure 10: Sequencing result when T-bet reverse primer was used.**

**Table 3: Alignment of sequencing result of T-bet reverse primer by performing a BLAST search.**

| Description                         | Max score | Total score | Query cover | E value | Ident | Accession   |
|-------------------------------------|-----------|-------------|-------------|---------|-------|-------------|
| Homo sapiens T-box 21 (T-bet), mRNA | 180       | 180         | 88%         | 1e-44   | 97%   | NM_013351.1 |

Table 3 demonstrates that the sequencing result of T-bet reverse primer was 97% identical to the Homo sapiens T-bet mRNA and covered 88% of it.

Supplementary figures 2-7 show the sequencing results of the other primers that were used in the differentiation assay. Supplementary table 1 demonstrates the BLAST alignment results of these sequencing results.

These data show that all primers were functional and amplified the correct sequence.

### 7.2.2 Gene expression after differentiation cocktails

After testing the functionality of the primers, the differentiation assay test was started. CD4+CD45RO+ T cells and CD14+ cells were isolated from PBMCs, after which they were co-cultured. This test was performed in duplo in which a differentiation cocktail was added to the co-culture for either Th1, Th2, or Th17 differentiation (see section 6.4.3) to determine the amount of gene expression when adding pure differentiating cytokines, and to see whether the differentiation assay was functional.

First, melt curves from the co-culture samples by means of qPCR were obtained (see section 6.4.3.1) (figure 11). No additional peaks in all melt curves that might suggest primer dimer formations or other non-specific amplification were found (figure 11 A-F).

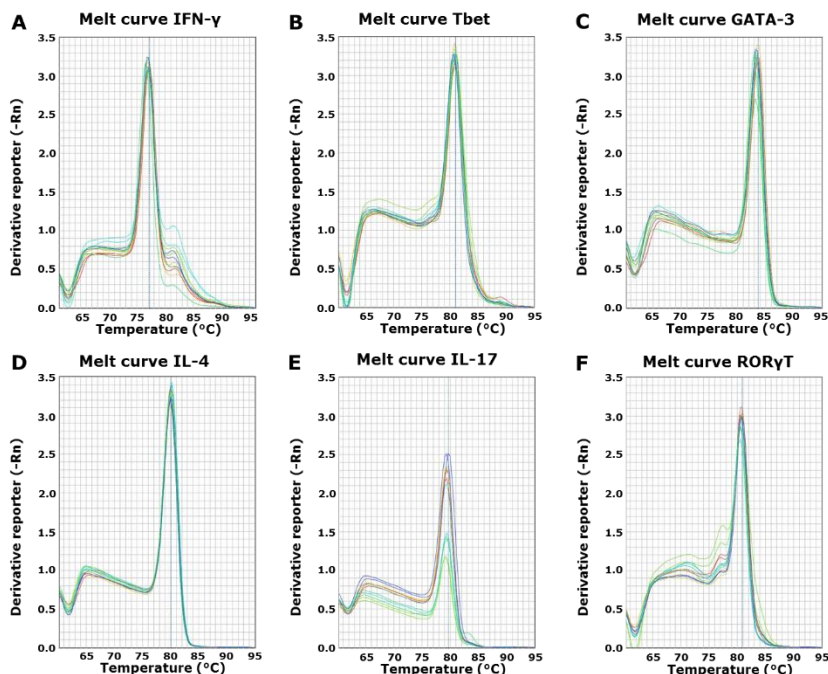


**Figure 11: Melt curves of the primers obtained after qPCR.** The same primers (see table 2) as in the differentiation assay were used. The melt curves of IFN- $\gamma$  (A), T-bet (B), GATA-3 (C), IL-4 (D), IL-17 (E), ROR $\gamma$ T (F) show no non-specific amplification peaks. GATA-3: Trans-acting T-cell-specific transcription factor; IL-4: Interleukin-4; ROR $\gamma$ T: RAR-related orphan receptor gamma T; IL-17: Interleukin-17; T-bet: T-box transcription factor TBX21; IFN- $\gamma$ : Interferon gamma.

Next, gene expression was measured by means of qPCR. In figure 12 the relative expression of the genes with respect to which differentiation cocktail was used can be observed.

When measuring the Th2 genes GATA-3 and IL-4 (figure 12 A and B), no difference in gene expression when using the differentiation cocktails can be observed. In the Th1 genes IFN- $\gamma$  and T-bet however, a clear increase in gene expression when using the Th1 differentiating cocktail is noticed (figure 12 C and D).

In figure 12 E and F, the Th17 genes ROR $\gamma$ T and IL-17 are measured, an increase in gene expression when using the Th17 differentiation cocktail can be seen.

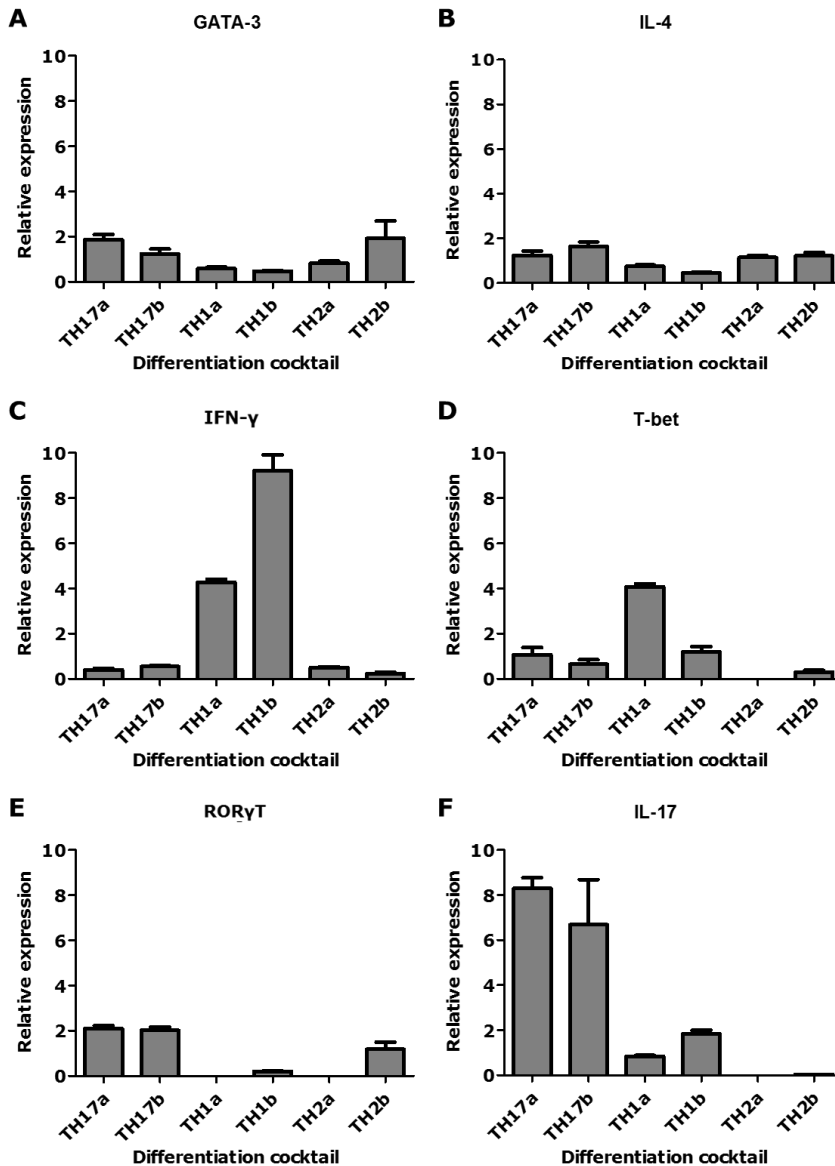


**Figure 12: Relative gene expression of (A) GATA-3, (B) IL-4, (C) IFN- $\gamma$ , (D) T-bet, (E) ROR $\gamma$ T, (F) IL-17 with respect to the differentiation cocktail used.** CD4<sup>+</sup>CD45RO<sup>+</sup> T cells and CD14<sup>+</sup> cells were isolated from PBMCs, after which they were co-cultured. Differentiation cocktails for Th1, Th2 and Th17 differentiation were added. Test was performed in duplo (Th1a, Th1b, Th2a, Th2b, Th17a, Th17b). Gene expression was measured by means of q PCR.

PBMC: Peripheral blood mononuclear cell; Th1: Type 1 helper T cell; Th2: Type 2 helper T cell; Th17: Type 17 helper T cell; GATA-3: Trans-acting T-cell-specific transcription factor; IL-4: Interleukin-4; ROR $\gamma$ T: RAR-related orphan receptor gamma T; IL-17: Interleukin-17; T-bet: T-box transcription factor TBX21; IFN $\gamma$ : Interferon gamma.

### 7.3 EAE study to determine the *in vivo* presence of CD4+CD28null T cells

After having determined several characteristics of the CD4+CD28null T cells *in vitro*, our research group wanted to investigate this cell subset *in vivo*. Since CD4+CD28null T cells are hypothesized to originate due to chronic inflammation and play an immunological role in MS, an EAE pilot study was set up (see section 6.5.1). In this study our research group wanted to determine if the number of CD4+CD28null T cells rise during disease progression and worsen the disease outcome. Furthermore immunohistochemistry was optimized to be able to localize the CD4+CD28null T cells in the spinal cord of the EAE mice in the future.

The data acquired from the three EAE groups (one group was sacrificed after 30 days, one after 60 days, and one after 90 days) were combined to form one EAE group.

The mice were followed up daily, by means of EAE scores (scoring performed according to table 2s) and weights (figure 13).

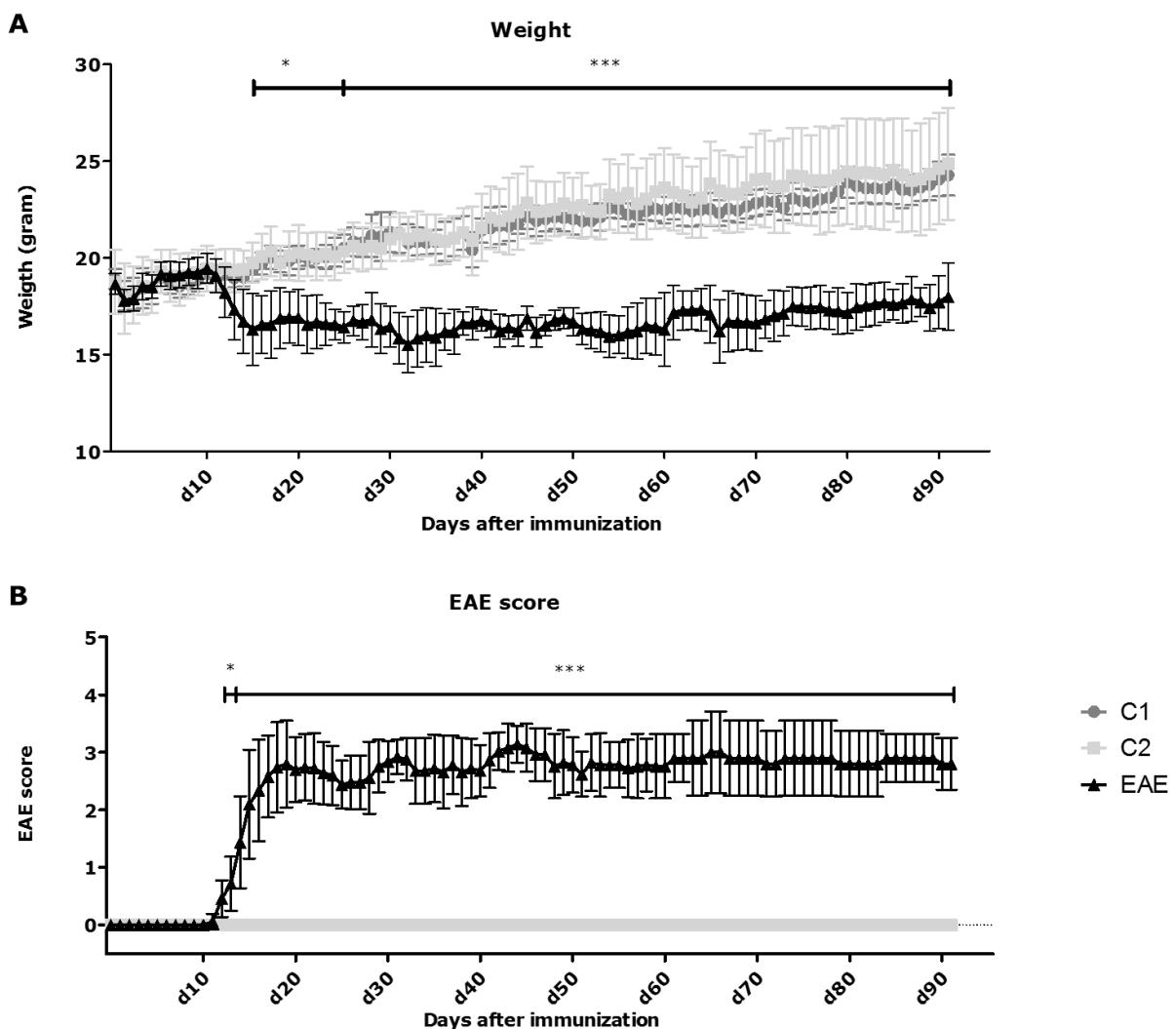


**Figure 13: Weight (A) and EAE score (B) of the mice for the whole duration of the EAE model.** Mice were divided into 2 control groups (C1 and C2; n=5 for each group) and 1 combined EAE group (n=15). Two way ANOVA was performed to find statistical differences in the cell percentage between groups (\*: P < 0.05; \*\*\*: P < 0.0001). C1= control group 1 that only received a CFA injection; C2= control group 2 that received a CFA and PTX injection; EAE= combined EAE group that received a CFA, PTX and MOG<sub>35-55</sub> injection. \*: P<0.05; \*\*\*: p<0.001.

The weight of the combined EAE group shows a decrease, while the control groups (C1 and C2) show an increase in weight (figure 13 A). The weight of the combined EAE group and both control groups start to significantly differ 15 days after immunization ( $P < 0.05$ ), after day 25 this significant difference is increased to  $P < 0.001$ . When looking at figure 14 B, one can see that the EAE scores of the C1 and C2 groups stay 0 for the whole duration of the experiment, while the score of the combined EAE group start to increase 10 days after immunization. A significant difference between the combined EAE group and both control groups can be found after d13 ( $P < 0.05$ ), after day 14 the significant difference is increased to  $P < 0.001$ .

To determine whether CD4+CD28null T cells aggravate EAE, the frequency of the CD4+CD28null T cells in the peripheral blood of the two control groups (C1 and C2) and the combined EAE group was determined (figure 14 A). Time points of CD4+CD28null T cell measuring were indicated with arrows on figure 14 B, which shows the EAE score during the first 50 days of the EAE study.

A trend of an increasing number of CD4+CD28null T cells is seen in the combined EAE group, which after day 17 changes to a decreasing trend (figure 14 A). At day 17 after immunization a significant difference in the number of CD4+CD28null T cells can be observed between C1 and the combined EAE group ( $P < 0.05$ ).

When looking at the arrows in figure 14 B, at day 17 the EAE scores are increasing towards a peak. At day 31 another peak in EAE score is reached. At day 45 another peak in EAE score is over and scores are gradually decreasing.

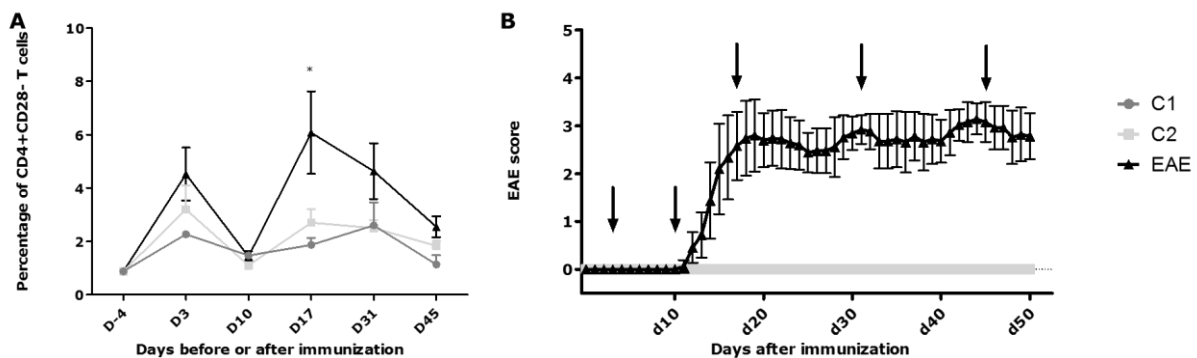


**Figure 14: (A) The percentage of CD4+CD28null T cells in the peripheral blood of the mice. (B) EAE score during the first 50 days of the study.** (B) Arrows indicate when CD4+CD28null T cell measurement occurred. Two way ANOVA was performed to find statistical differences in the cell percentage between groups (\*:  $P < 0.05$ ). C1= control group 1 that only received a CFA injection; C2= control group 2 that received a CFA and PTX injection; EAE= combined EAE group that received a CFA, PTX and MOG<sub>35-55</sub> injection.

Since figure 14 showed that a correlation between CD4+CD28null T cell percentage and EAE score may be possible, the frequency of CD4+CD28null T cells with respect to EAE score was plotted (figure 15). At an EAE score of 0 the CD4+CD28null T cell subset percentage ranges from 0 – 5%, with a few outliers. The spearman R was calculated and a linear regression was fitted to calculate the correlation between CD4+CD28null T cells and EAE score. When EAE scores increases higher numbers of CD4+CD28null T cells are present ( $P < 0.0001$ ).

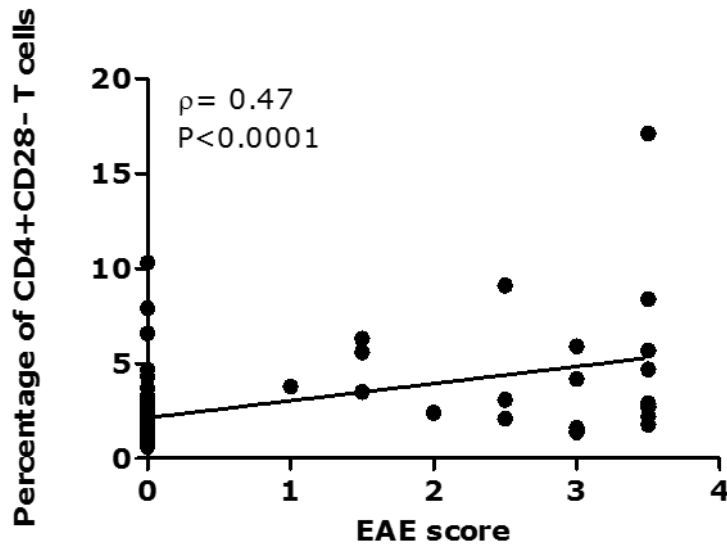


**Figure 15: Percentage of CD4+CD28null T cells compared to EAE scores.** Peripheral blood was drawn retro-orbitally, the number of CD4+CD28null T cells was analyzed by flow cytometry. Linear regression calculated the increase of CD4+CD28null T cells with elevating EAE scores ( $P < 0.0001$ ).  $\rho$  = spearman r correlation.

Data from figure 15 suggests that the number of CD4+CD28null T cells increases with EAE score, and hence may contribute to the aggravation of EAE.

Phenotypic markers of the CD4+CD28null T cell subset were also measured at different days before or after immunization (figure 16 A-E).

When looking at several relevant markers, we can see a trend of decreasing CD27+ cells within the CD4+CD28null T cell population in all observed groups (figure 16 A). The percentage of CD4+CD28null CD27+ T cells significantly differ at day 10 after immunization between C1 and the combined EAE group ( $P < 0.05$ ). The same decreasing trend can be noticed when looking at the CD62L+ within the CD4+CD28null T cell population (figure 16 B). No significant differences between groups can be noticed for this cell subset.

If we look at the CD4+CD28null CD127+ T cells (figure 16 C), a decreasing trend can be noticed in both control groups, and an increasing trend can be observed in the combined EAE group. A significant difference of the CD4+CD28null CD127+ T cells between C2 and the combined EAE group can be observed at day 31 ( $P < 0.01$ ). An increasing trend can be observed when looking at the NKG2D+ and IFN- $\gamma$ + cells within the CD4+CD28null T cell population (figure 16 D-E). No significant differences in both cell subsets between the three groups could be found.

These data show that CD4+CD28null T cells increase in the combined EAE group over time and that several naïve T cell markers such as CD27, CD62L decrease over time within the CD4+CD28null T cell population.

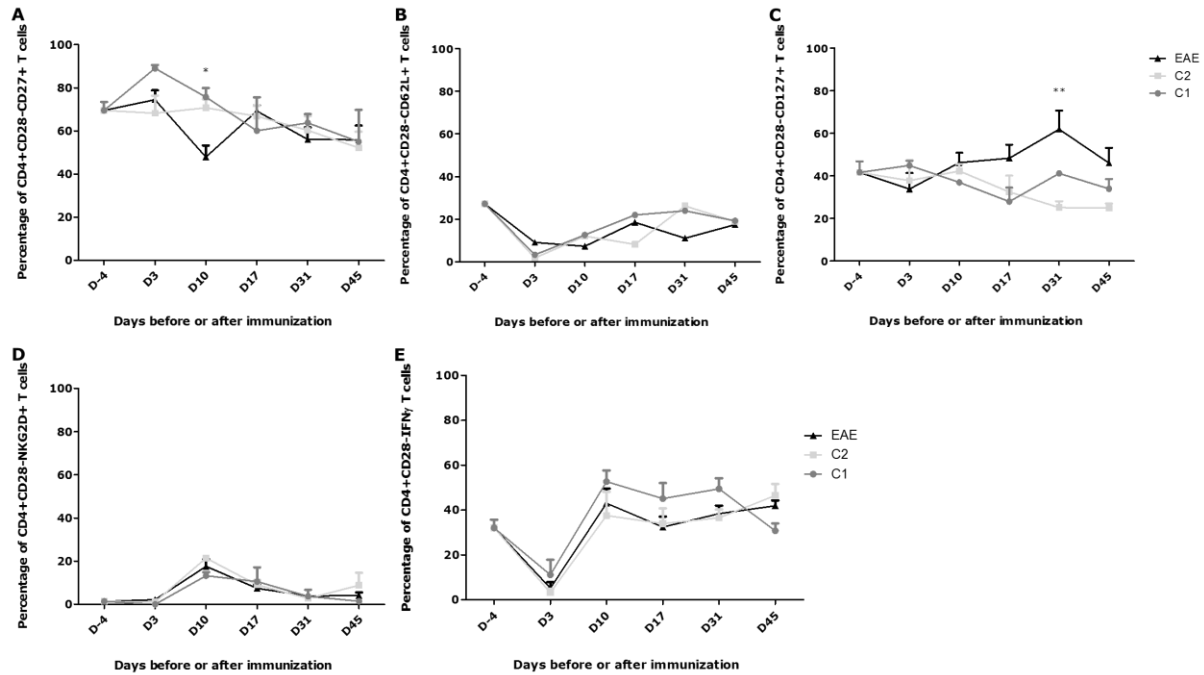


**Figure 16: Phenotypic markers of the CD4+CD28null T cells measured at different days before and after immunization.** (A) Percentage of CD4+CD28null CD27+ T cells. (B) CD4+CD28null CD62L+ T cell percentage. (C) CD4+CD28null CD127+ T cell population percentage. (D) Percentage of CD4+CD28null NKG2D+ T cells. (E) The number of CD4+CD28null IFN- $\gamma$ + T cells. Two way ANOVA was performed to find statistical differences in the cell percentage between groups (\*:  $P < 0.05$ ; \*\*:  $P < 0.01$ ). C1= control group 1 that only received a CFA injection; C2= control group 2 that received a CFA and PTX injection; EAE= combined EAE group that received a CFA, PTX and MOG<sub>35-55</sub> injection. CD28: cluster of differentiation 28; CD27: cluster of differentiation 27; CD62L: L-selectin; CD127: cluster of differentiation 127; NKG2D: natural killer group 2, member D; IFN- $\gamma$ : interferon  $\gamma$ . \*:  $P < 0.05$ ; \*\*:  $P < 0.01$ .

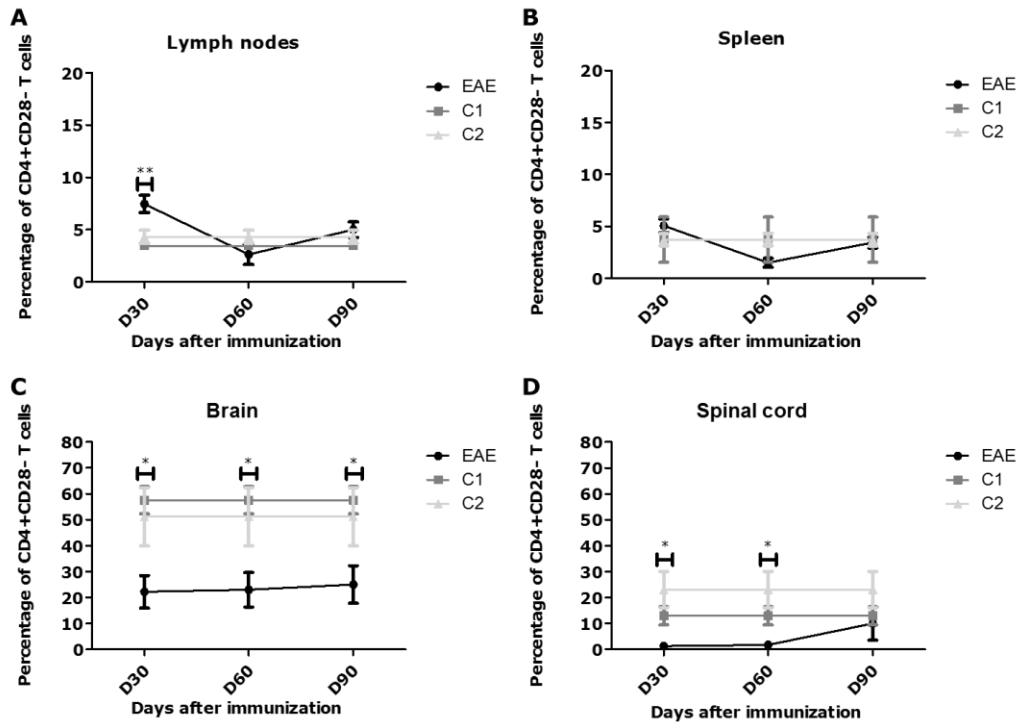
Next to determining the frequency of the CD4+CD28null T cells together with their relevant markers in the peripheral blood of mice, the CD4+CD28null T cell percentage was determined in several organs (figure 17). This was accomplished by making cell suspensions of isolated organs (see section 6.5.2). The frequency of CD4+CD28null T cells was determined by flow cytometry analysis (see section 6.5.3).

Figure 18 A shows the percentage of CD4+CD28null T cells isolated from lymph nodes. In the combined EAE group the number of CD4+CD28null T cells show a decreasing trend toward day 90 after immunization. At day 30 after immunization a significant difference between the combined EAE group and C1 group ( $P < 0.001$ ), and the combined EAE group and C2 group ( $P < 0.01$ ) can be found.

No upward or downward trend can be observed when looking at the CD4+CD28null T cells isolated from the spleen (figure 17 B), also no significant differences between groups can be found.

Figure 17 C shows the CD4+CD28null T cell subset isolated from the brain, a slight increasing trend can be observed in the combined EAE group. At day 30, 60 and 90 after immunization a significant difference between cell percentages can be found between the combined EAE and C1 group ( $P < 0.01$  at day 30,  $P < 0.01$  at day 60, and  $P < 0.05$  at day 90), another significant difference can be noted between the combined EAE and C2 group at day 30 and 60 ( $P < 0.05$ ).

An increasing trend can be observed in the CD4+CD28null T cells isolated from the spinal cord from the combined EAE group (figure 17 D). CD4+CD28null T cell percentages significantly differ between the combined EAE and C2 group at day 30 and 60 after immunization ( $P < 0.05$ ).



**Figure 17: Percentage of CD4+CD28null T cells isolated from (A) lymph nodes, (B) spleen, (C) brain, and (D) spinal cord.** (A) A significant difference can be found between the EAE and C1 group ( $P < 0.001$ ), and the EAE and C2 group ( $P < 0.01$ ). (B) No significant differences between groups can be detected. (C) At D30, D60, D90 the percentage of CD4+CD28null T cells significantly differ between the EAE and C1 group ( $P < 0.01$  at D30,  $P < 0.01$  at D60, and  $P < 0.05$  at D90), at D30 and D60 the cell percentage significantly differs between the EAE group and C2 group ( $P < 0.05$ ). (D) A significant difference in the percentage of CD4+CD28null T cells can be found between the EAE and C2 group ( $P < 0.05$ ). C1= control group 1 that only received a CFA injection; C2= control group 2 that received a CFA and PTX injection; EAE= combined EAE group that received a CFA, PTX and MOG<sub>35-55</sub> injection. \*:  $P < 0.05$ ; \*\*:  $P < 0.01$ .

After determining the number of CD4+CD28null T cells in the lymph nodes, spleen, brain and spinal cord, immunohistochemistry on spinal cord slides of EAE mice was optimized to be able to localize the CD4+CD28null T cell subset (figure 18).

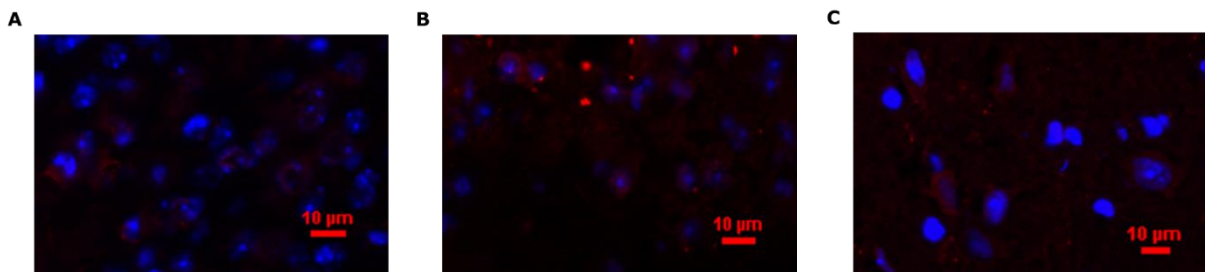


**Figure 18: Immunohistochemistry spinal cord slides stained with (A) CX<sub>3</sub>CR1, (B) CD3, or (C) CD4.** EAE mice were sacrificed and spinal cord was isolated and sliced. Slides were stained with DAPI. CX<sub>3</sub>CR1, CD3, or CD4 were used as primary antibody and alexa fluor 555 as secondary antibody. Magnification: 40x. Scale bar: 10μM. DAPI: 4',6-diamidino-2-phenylindole; CX<sub>3</sub>CR1: fractalkine receptor; CD3: cluster of differentiation 3; CD4: cluster of differentiation 4.

The spinal cord was either stained with CX<sub>3</sub>CR1, CD3, or CD4 (figure 18 A-C). Each staining showed a clear fluorescent signal circulating some of the cells, suggesting that these cells contain the protein of interest.

These data suggest the presence of CX<sub>3</sub>CR1+, CD3+, and CD4+ cells in the spinal cord of EAE mice.

## 8 Discussion

Our research group hypothesized that CD4+CD28null T cells originated due to chronic CMV stimulation and that they can induce an immune response towards auto-antigens and MS relevant cells such as oligodendrocytes and astrocytes.

In order to see the distribution of CD4+CD28null T cells in HC and MS donors, the percentage of CD4+CD28null T cells was measured (figure 3). Data from figure 3 showed that 18.9% of the HC and 27.9% of the MS donors had a CD4+CD28null T cell expansion. This is in accordance with findings in other research, which found an expansion of the CD4+CD28null T cell subset in 20% of the MS and HC donors (27).

The reactivity of the CD4+CD28null T cells against MBP was determined (figure 4). This study demonstrated that the percentage of CD4+CD28null T cells in MBP reactive T cell clones increased after several rounds of stimulation with MBP and PHA, showing that a proportion of the CD4+CD28null T cell subset indeed is reactive against an auto-antigen, which may suggest that these cells can play a role in MS pathology. Markovic-Plese et al. already suggested that a proportion of CD4+CD28null T cells are reactive against MBP (19).

Research also has shown that the CD4+CD28null T cells can play a role in other chronic inflammatory diseases, such as rheumatoid arthritis, Wegener's granulomatosis, Graves' disease (19, 22, 23, 28, 39, 40).

Several experiments were conducted to provide evidence for the origin of the CD4+CD28null T cell subset. The data from the first CMV assay (figure 5) demonstrated that the number of CD4+CD28null T cells increased after chronic stimulation with CMV pp65, IL-2, and with CMV+IL-2 in the CMV+/Exp+ donor. However, this number did not increase in the CMV+/Exp- and CMV-/Exp- donors. Our research group expected to see an increase in the number of CD4+CD28null T cells from the CMV+/Exp+ donor in each stimulatory condition. However, we also expected to see a higher increase of the CD4+CD28null T cells in the CMV and CMV+IL-2 stimulatory condition in the CMV+/Exp+ donor. Since this donor was CMV seropositive and already had an CD4+CD28null T cell expansion, the CD4+CD28null T cells would have already been in contact with the CMV antigen and thus proliferate more rapidly when encountering the antigen again. Indeed research has shown that the CD4+CD28null T cell subset reacts to CMV (29, 34, 35). We also expected to see an increase in the CD4+CD28null T cell percentage in the other donors in the IL-2 stimulatory condition, which did not occur. Since IL-2 is an important interleukin in T cell proliferation, the CD4+CD28null T cell fraction should have proliferated (41).

In the CMV+/Exp- donor we expected to see a higher increase in the number of CD4+CD28null T cells in the CMV+IL-2 condition compared to the IL-2 condition, because in this donor the CMV antigen was already present and thus other immune cells than the CD4+CD28null T cells would react when encountering this antigen again and could stimulate the CD4+CD28null T cells to proliferate.

The only way to be able to conclude that the CD4+CD28null T cells find their origin in chronic CMV stimulation was if the CMV-/Exp- donor showed an increase in this cell subset after CMV stimulation. This increase did not occur in this experiment. However, out of this data we can conclude that the

CD4+CD28null T cells react to CMV, and chronic CMV stimulation can induce the proliferation of this cell subset.

The CMV assay was repeated (figure 6) to confirm the results seen in the first CMV assay, and to see if the unexpected observations discussed above occurred once more. The data from this CMV assay showed that the CD4+CD28null T cells from the CMV+/Exp+ donor again increased after stimulation with either IL-2, CMV or CMV+IL-2. In this assay also the CD4+CD28null T cells from the CMV-/Exp- donor surprisingly increased with every stimulatory condition. The number of CD4+CD28null T cells from the CMV-/Exp- donor even surpassed the number of CD4+CD28null T cells from the CMV+/Exp+ donor in the IL-2 stimulatory condition, which was not expected at all since the number of CD4+CD28null T cells in the beginning of the experiment were very low in the CMV-/Exp- donor and very high in the CMV+/Exp+ donor and that with the administration of IL-2 the number of cells should increase only gradually. The CD4+CD28null T cell percentage from donor CMV+/Exp- did not vary in each stimulatory condition.

In conclusion, the data from this experiment demonstrates that CD4+CD28null T cells are reactive to CMV and may find their origin in the chronic stimulation of CMV since the CMV-/Exp- donor showed an increase in CD4+CD28null T cells in the CMV and CMV+IL-2 stimulatory conditions.

Data from both CMV assays conducted in this study and from a preliminary CMV assay were combined to create a more accurate result (figure 7). This data shows that in the IL-2 stimulatory condition the CD4+CD28null T cells from all donors increase, which was expected as mentioned above. Furthermore this data demonstrates that the CD4+CD28null T cells from the CMV+/Exp+ and CMV+/Exp- donor rise in the CMV+IL-2 stimulatory condition, while in the CMV-/Exp- donor the percentage of CD4+CD28null T cells do not rise. As discussed above, this is due to the fact that the immune cells of the CMV+ donors already have been in contact with the CMV antigen before, and when encountering the antigen again a larger response will be formed.

Moreover this data shows that in a CMV stimulatory condition only the CD4+CD28null T cells of the CMV+/Exp+ donor increases.

Altogether these data demonstrate that the CD4+CD28null T cell subset is reactive to CMV stimulation. However the origin of these cells is probably not due to chronic stimulation of CMV.

An issue with the CMV assays however is that the increases in the CD4+CD28null T cell population that is seen several days after culturing and stimulating the cells may not be due to proliferation of the cell subset itself, but may be due to a switch from CD4+CD28+ T cells to CD4+CD28null T cells. This issue should be addressed when performing other CMV assays in the future. One probable solution is to label the CD4+CD28null T cells with CFSE during the experiment.

During the CMV assays other surface markers, such as CD45RO (supplementary figure 1) and CD45RA (figure 8), were measured together with the total number of CD4+CD28null T cells. CD45RO is a memory T cell marker, while CD45RA is a marker for naïve T cells (19, 24). These surface markers were measured to confirm the results that were found in other research, which showed that the CD4+CD28null T cell subset is a memory cell subset (19, 23-25, 35, 42). Data from supplementary figure 1 showed that from the start of the experiment (day 0) the percentage of

CD45RO+ cells within the CD4+CD28null T cells are very high, varying from 40 to 80%. After stimulation with either CMV, IL-2, or CMV+IL-2 the CD45RO+ population increases in each donor. At the end of the experiment (day 20) the percentage of CD45RO+ cells within the CD4+CD28null T cell population ranges between 85 and 99%.

One exception is seen in the CMV stimulatory condition in the CMV+/Exp- donor, which shows a decreasing trend of CD45RO+ cell towards the end of the experiment. A possible explanation for this is that at day 15 and day 20 a very few number of cells were measured by flow cytometric analysis and hence the proportion might be shifted.

Data from figure 8 demonstrated that at the beginning of the experiment a relatively low number of CD45RA+ cells within the CD4+CD28null T cell population can be found, the number varying from 10 to 40%. In all stimulatory conditions (IL-2, CMV, CMV+IL-2) and in all donors, a decrease in CD45RA+ cells when progressing to the end of the experiment can be noted. When looking at day 20 of the experiment the percentage of CD45RA+ cells within the CD4+CD28null T cell population varies between 0 and 8.5%.

The same exception is found when looking at the CMV+/Exp- donor in the CMV stimulatory condition, which shows an increasing trend of CD45RA+ towards the end of the experiment.

Taken together the data from figure 8 and supplementary figure 1 show that the CD4+CD28null T cell population clearly is a memory T cell population and stimulation with CMV, IL-2, or CMV+IL-2 shifts the balance of these cells to an even more memory like population.

Our research group wanted to determine another characteristic of the CD4+CD28null T cells, namely the differentiating capacity. This would be determined by using a Th differentiation assay. In this assay the supernatant from CD4+CD28null T cells would be used to stimulate a co-culture of CD4+CD45RO+ T cells and CD14+ cells. However only the optimization of this assay was performed in this study due to a limited amount of time. This optimization included testing the primers for their functionality by either gel electrophoresis (figure 9), sequencing (figure 10 + table 3, and supplementary figures 2-7 + supplementary table 1), and qPCR (figure 11). Data from figure 9 showed us that the bands from the agarose gel were at the correct height, corresponding with the correct length of the amplicon (see table 2). The length of the amplicons was obtained by performing a BLAST search. This data suggested that the primers that were used amplified the correct sequence. Figure 10 demonstrates that sequencing result that was obtained when using the T-bet reverse primer. When performing an alignment of this sequence on BLAST a near perfect match with the correct target sequence is obtained (table 3). The other primers that were used in the differentiation assay were sequenced as well (supplementary figures 2-7 + supplementary table 1), again a near perfect match with the correct target sequence was obtained.

The data from figure 11 demonstrated the melt curves from the primers that were used obtained after a qPCR. No additional peaks in the curves were observed, which meant that no non-specific byproducts such as primer dimer formations were amplified.

Together the data from figure 9, figure 10 + table 3, supplementary figures 2-7 + supplementary table 1, and figure 11 show us that the primers that are used in the differentiation assay work properly and amplify the correct sequence.

After testing the functionality of the primers a first differentiation assay test was performed (figure 12). In this test multiple cytokines specific for a certain Th differentiation (Th1, Th2, or Th17) were

added to the co-culture of CD4<sup>+</sup>CD45RO<sup>+</sup> T cells and CD14<sup>+</sup> cells to cause Th1, Th2, and Th17 differentiation (see section 6.4). This was done to have an idea about the gene expression pure differentiation cytokines would induce. Data from figure 12 demonstrated that the differentiation cocktail used for Th1 and Th17 differentiation caused an increase in the Th1 and Th17 gene expression. However the increase in Th2 gene expression could not be observed when the Th2 differentiation cocktail was used. This indicates that further optimization with respect to Th2 differentiation is needed, including the adjustment of the concentration of differentiation cytokines that are added to the co-culture.

Beside *in vitro* experiments this study also included an *in vivo* experiment, in which mice were immunized with EAE. This experiment was performed to see if the CD4<sup>+</sup>CD28null T cell subset was present in the blood and organs of EAE mice, and if these cells would aggravate the disease. Which would bring us one step closer to linking the CD4<sup>+</sup>CD28null T cells with MS pathology.

The data from figure 13 demonstrate that all mice from the EAE group showed the first symptoms of disease 10 days after immunization, while the mice from both control groups showed no symptoms at all. At the same time the mice from the EAE group gradually lost weight, while the mice from both control groups gained weight. This indicates that there was no difference in weight or EAE scores between both control groups, while the C1 group only received a CFA injection and the C2 group received a CFA and PTX injection at the start of the EAE study. Furthermore this data indicated that EAE immunization was successful. Even 90 days after immunization the EAE course kept constant, while in the manufacturers' protocol the course is only described up to 30 days (Hooke Laboratories, EAE induction by active immunization in C57BL/6 mice).

To determine if the CD4<sup>+</sup>CD28null T cells aggravate the course of EAE, the cell percentage was measured in the peripheral blood of mice (figure 14 A). Time points when CD4<sup>+</sup>CD28null T cells were measured were indicated with arrows on the EAE course (figure 14 B). At day 10 a low amount of CD4<sup>+</sup>CD28null T cells is measured in the peripheral blood, while at day 10 the EAE score still is 0. This may indicate that CD4<sup>+</sup>CD28null T cells from the peripheral blood moved towards the spinal cord and brain and started the EAE pathology, because a few days later EAE scores increased. At day 17 a high amount of CD4<sup>+</sup>CD28null T cells is measured in the peripheral blood, and at the same day a higher EAE scores are measured. This suggests that CD4<sup>+</sup>CD28null T cells maybe are proliferating to prepare for a new immune response. At day 31 a peak in EAE score is measured, while still a high amount of CD4<sup>+</sup>CD28null T cells are in the peripheral blood and in the spleen (figure 17 B) and lymph nodes (figure 17 A), this possibly indicates that these cells are priming other immune cells to mount an immune response. At day 45 a low amount of CD4<sup>+</sup>CD28null T cells is measured in the peripheral blood, while a peak in EAE score has passed a few days earlier. This possibly suggests that these cells are still in the spinal cord and brain causing EAE pathology.

Data from figure 14 demonstrated that there may be a correlation between the number of CD4<sup>+</sup>CD28null T cells and EAE score.

The correlation between CD4<sup>+</sup>CD28null T cell percentage and EAE score was shown in figure 15. This data demonstrated that the number of CD4<sup>+</sup>CD28null T cells increased with increasing EAE scores, which suggests that CD4<sup>+</sup>CD28null T cells can cause a worsening of the disease.

Data from figure 16 showed further phenotyping of the CD4+CD28null T cell population with several markers such as CD27, CD62L, CD127, NKG2D, and IFN- $\gamma$ , measured within this general population. We could notice that the general CD4+CD28null T cell population increased in the combined EAE group, while remaining at the same level in both control groups. This result was expected since CD4+CD28null T cells are known to proliferate and originate out of a pro inflammatory environment (22, 23, 31, 33), like EAE.

Furthermore this data showed that the CD27+ cells within the CD4+CD28null T cell population was decreasing over time in all groups. Since we are looking within the CD4+CD28null T cell population we expect to see a low amount of CD27+ T cells in all groups. We expected to see a gradual decrease in the number of CD27+ cells in the combined EAE group, because CD27 is a co-stimulatory molecule that is lost in highly differentiated CD4+CD28null T cells (22, 29, 34, 43, 44). However we did not expect to see the number of CD27+ cell gradually decrease in the control groups, since there is no continuous inflammation going on in these groups, thus no further differentiation of the CD4+CD28null T cell subset should occur.

Figure 16 also demonstrated that there was a slight decrease in CD62L+ cells in all groups within the CD4+CD28null T cell population. Since CD62L+ is a homing receptor to secondary lymphoid organs, and the CD4+CD28null T cells are considered to be a memory T cell subset, we did expect to find a decrease of CD62L+ cells over time. Duftner et al. and Broux et al. also showed that the CD62L protein is downregulated in the CD4+CD28null T cell subset (27, 45). The same issue arose as with the CD27 marker, namely we saw a gradual decrease in all groups, while we only expected it to see in the combined EAE group.

A decrease in the number of CD127+ cells within the CD4+CD28null T cell population is found for both control groups, while an increase of these cells can be noted in the combined EAE group. Our expectations were to see a decrease of the CD4+CD28null CD127+ T cell percentage, since CD127 plays a role in the maturation of T cells and the CD4+CD28null T cells are fully matured (46). *In vitro* experiments have shown that the CD127 protein decreases in CD4+CD28null T cells after stimulation (27, 47). We did not expect to see an increase of the CD127 protein over time in the combined EAE group, we also expected to see a steady number of CD4+CD28null CD127+ T cells in the control groups.

Another observation made from figure 16 is that the number of NKG2D+ cells within the CD4+CD28null T cell population does not vary during the experiment except the increase on day 10 in all groups. The percentage of CD4+CD28null NKG2D+ T cells at the beginning of the experiment was very low, our research group expected to see a high number of NKG2D+ cells within the CD4+CD28null T cell population, because according to Broux et al. (23) NKG2D expression is mainly linked to CD4+CD28null T cells. Other research confirmed that CD4+CD28null T cells have an upregulation of this receptor (20-22, 24, 26). We also expected to see an increase of the NKG2D+ cells in the combined EAE group over time, which did not occur.

Lastly, data from figure 16 demonstrated an increase of CD4+CD28null IFN- $\gamma$ + T cells during the experiment in all groups, except for the decrease at day 3. A high percentage of these cells are expected to be present, since many studies have revealed that CD4+CD28null T cells are potent IFN- $\gamma$  producing cells (21, 24-26, 48). Our research group also expected to see an increase of these cells during the experiment in the combined EAE group, since in this group the CD4+CD28null T cells are

experiencing chronic inflammation. For the same reason we did not expect to see an increase of the CD4+CD28null IFN- $\gamma$ + T cells in the control groups.

Taken together the data from figure 16 demonstrates that CD4+CD28null T cell subset is increased in the combined EAE group, and thus might contribute to the EAE pathophysiology. This data also showed that the CD4+CD28null T cells lose naïve receptors, such as CD62L, co-stimulatory receptors, like CD27, and gain effector molecules, such as IFN- $\gamma$  when exposed to an inflammatory condition like EAE. However also unexpected findings were observed, such as the raise in the CD127 protein in the combined EAE group and the low number of CD4+CD28null NKG2D+ T cells in all groups. These unexpected findings may be resolved by repeating the EAE model with a larger sample size, since this EAE model was a pilot study.

As mentioned above we did not only measured CD4+CD28null T cells in the blood in the EAE model, we also measured these cells in lymph nodes, spleen, brain, and spinal cord. Data from figure 17 show that CD4+CD28null T cells from the combined EAE group isolated from lymph nodes show a decreasing pattern towards the end of the experiment. These cells also are increased at d30 in comparison with the control groups.

These data also show a slight decreasing pattern of CD4+CD28null T cells from the combined EAE group derived from the spleen. The number of CD4+CD28null T cells from the combined EAE group does not vary from the number of cells in the control groups.

Data from figure 17 shows a high number of CD4+CD28null T cells from the control groups present in the brain, while the number of cells is lower in the combined EAE group but slightly increases towards the end of the experiment. We did not expect to see such a high number of CD4+CD28null T cells in the control groups, this high percentage might be due to the fact that during the flow cytometric analysis very few cells were counted which leads to a shift in the proportion of CD4+CD28null vs CD4+CD28+ T cells.

A high number of spinal cord derived CD4+CD28null T cells from the control groups can be seen. More CD4+CD28null T cells in the control groups than in the combined EAE group can be observed. The CD4+CD28null T cells from the combined EAE group slightly increase during the experiment. Our research group also did not expect to see a higher number of CD4+CD28null T cells in the control group than in the combined EAE group, this high percentage again may be caused by the fact that very few cells were counted during the flow cytometric analysis. We also expected to see a higher number of the CD4+CD28null T cells from the combined EAE group at day 30 after immunization, since in EAE the spinal cord is affected and at day 30 EAE scores are increased to a score of 2.5-3, which means the hind limbs of the mice are almost or completely paralyzed.

Taken together data from figure 17 suggests that the CD4+CD28null T cell percentage decreases in the lymph nodes and spleen in the combined EAE group during the course of the EAE model, while the number increases gradually over time in the brain and spinal cord. This suggests that CD4+CD28null T cells gradually move from the spleen and lymph nodes to brain and spinal cord to cause EAE pathology. One issue in this model was the low cell number measurement by flow cytometric analysis of the CD4+CD28null T cells in the brain and spinal cord of the mice. This problem may be solved by repeating the EAE model with a bigger sample size, because this EAE model was a pilot study.

Immunohistochemistry was optimized to be able to stain for CD4+CD28null T cells in spinal cord tissue of EAE mice. Anti-CX<sub>3</sub>CR1, anti-CD3, and anti-CD4 were chosen as primary antibodies for eventual CD4+CD28null T cell staining. Anti-CX<sub>3</sub>CR1 is used as a primary antibody, since CX<sub>3</sub>CR1 is limited to CD4+CD28null T cells compared to CD4+CD28+ T cells, however CX<sub>3</sub>CR1 is also expressed by other cell types than CD4+CD28null T cells (27), which is why also other primary antibodies are chosen. Anti-CD4 is used as a primary antibody, because CD4+ T cells have to be stained, however some cells, such as microglia also express the CD4 protein (49), which is why also anti-CD3 is chosen as a primary antibody. CD3 is a co-receptor only expressed on T lymphocytes (50).

Data from figure 18 demonstrated that the staining for CX<sub>3</sub>CR1, CD3, and CD4 proteins was successful and that these proteins are present on cells in the spinal cord of EAE mice. This indicates that the optimization of these stainings is complete, and that double or triple stainings can be performed in the future to localize the CD4+CD28null T cell subset.

In conclusion this study demonstrated that CD4+CD28null T cells may find their origin in the chronic stimulation by CMV, and that these cells are a memory cell subset that becomes more pronounced after chronic stimulation. Moreover we have demonstrated that a proportion of CD4+CD28null T cells are autoreactive.

This study has provided evidence for the existence of the CD4+CD28null T cell subset in an *in vivo* EAE mouse model. Furthermore our research group has shown that there is a correlation between the number of CD4+CD28null T cells and EAE score, suggesting that these cells play a role in EAE pathology.

This study also has led to further phenotyping of this cell subset in the *in vivo* EAE model, in which we could conclude that certain naïve and co-stimulatory markers decreased, while other effector molecules increased.

Immunohistochemical optimization was accomplished, which will enable us to localize the CD4+CD28null T cells in spinal cord tissue.

Certain aims were set in the beginning of this study. Our research group wanted to investigate the amount of degranulation of the CD4+CD28null T cells in the presence of MS relevant cells such as oligodendrocytes and astrocytes. We wanted to determine the differentiating capacities of the CD4+CD28null T cell subset. Although this aim was not accomplished our research group suspects that the CD4+CD28null T cells will differentiate other T cells to a Th1 phenotype, because research has shown that the CD4+CD28null T cells are IFN- $\gamma$  producing cells (21, 24-26, 48) and IFN- $\gamma$  drives Th1 differentiation (51). Our research group also wanted to conduct a genetic study to provide evidence for the origin of the CD4+CD28null T cells. In this genetic study we wanted to investigate if certain SNPs in the MicB (rs2523651) and TLR2 (rs5743708) genes increase the risk for CD4+CD28null T cell expansion, since these SNPs are associated with an increased risk of CMV infection (36-38). Because our research group has determined that chronic CMV infection may cause an expansion of the CD4+CD28null T cells, we suspect that people with the MicB and TLR2 SNPs will have a higher number of CD4+CD28null T cells.

However due to a limited amount of time these aims could not be accomplished in this study. Future research will determine the outcome of these aims. Furthermore a new EAE model with a larger sample size should be set up, which can lead to clearer and more significant results. Moreover the

results from the *in vitro* CMV data could be validated in a new EAE model, in which CMV seropositive mice are used.

## 9 References

1. Compston A, Coles A. Multiple sclerosis. *Lancet*. 2008;372(9648):1502-17.
2. van Noort JM. Antigen-specific therapies in multiple sclerosis. *Biotherapy*. 1998;10(3):237-50.
3. Minagar A, Alexander JS. Blood-brain barrier disruption in multiple sclerosis. *Multiple Sclerosis*. 2003;9(6):540-9.
4. Compston A, Coles A. Multiple sclerosis. *Lancet*. 2002;359(9313):1221-31.
5. Ascherio A, Munger KL. Environmental risk factors for multiple sclerosis. Part I: the role of infection. *Ann Neurol*. 2007;61(4):288-99.
6. Federation MSI. Atlas of MS 2013: Mapping multiple sclerosis around the world 2013. 28 p.
7. Organization WH. Atlas: Multiple sclerosis resources in the world 2008 2008. 51 p.
8. Polman CH, Reingold SC, Banwell B, Clanet M, Cohen JA, Filippi M, et al. Diagnostic Criteria for Multiple Sclerosis: 2010 Revisions to the McDonald Criteria. *Annals of Neurology*. 2011;69(2):292-302.
9. McDonald WI, Compston A, Edan G, Goodkin D, Hartung HP, Lublin FD, et al. Recommended diagnostic criteria for multiple sclerosis: Guidelines from the International Panel on the Diagnosis of Multiple Sclerosis. *Annals of Neurology*. 2001;50(1):121-7.
10. Hartung HP, Gonsette R, König N, Kwiecinski H, Guseo A, Morrissey SP, et al. Mitoxantrone in progressive multiple sclerosis: a placebo-controlled, double-blind, randomised, multicentre trial. *Lancet*. 2002;360(9350):2018-25.
11. McCormack PL, Scott LJ. Interferon-beta-1b - A review of its use in relapsing-remitting and secondary progressive multiple sclerosis. *Cns Drugs*. 2004;18(8):521-46.
12. Christophi GP, Christophi JA, Gruber RC, Mihai C, Mejico LJ, Massa PT, et al. Quantitative differences in the immunomodulatory effects of Rebif and Avonex in IFN-beta 1a treated multiple sclerosis patients. *Journal of the Neurological Sciences*. 2011;307(1-2):41-5.
13. Dhib-Jalbut S. Mechanisms of action of interferons and glatiramer acetate in multiple sclerosis. *Neurology*. 2002;58(8):S3-S9.
14. Dhib-Jalbut S. Glatiramer acetate (Copaxone (R)) therapy for multiple sclerosis. *Pharmacology & Therapeutics*. 2003;98(2):245-55.
15. Johnson KP, Brooks BR, Cohen JA, Ford CC, Goldstein J, Lisak RP, et al. Extended use of glatiramer acetate (Copaxone) is well tolerated and maintains its clinical effect on multiple sclerosis relapse rate and degree of disability. *Neurology*. 2001;57(12):S46-S53.
16. Yadav V, Bourdette D. New disease-modifying therapies and new challenges for MS. *Curr Neurol Neurosci Rep*. 2012;12(5):489-91.
17. Hopkins CR. ACS chemical neuroscience molecule spotlight on gilenya (fingolimod; FTY720). *ACS Chem Neurosci*. 2011;2(3):116-7.
18. Chanvillard C, Millward JM, Lozano M, Hamann I, Paul F, Zipp F, et al. Mitoxantrone Induces Natural Killer Cell Maturation in Patients with Secondary Progressive Multiple Sclerosis. *Plos One*. 2012;7(6).
19. Markovic-Plese S, Cortese I, Wandinger KP, McFarland HF, Martin R. CD4(+)CD28(-) costimulation-independent T cells in multiple sclerosis. *Journal of Clinical Investigation*. 2001;108(8):1185-94.
20. Thewissen M, Somers V, Venken K, Linsen L, Van Paassen P, Geusens P, et al. Analyses of immunosenescent markers in patients with autoimmune disease. *Clinical Immunology*. 2007;123(2):209-18.
21. Pawlik A, Ostanek L, Brzosko W, Brzosko M, Masiuk M, Machalinski B, et al. Therapy with infliximab decreases the CD4+ CD28- T cell compartment in peripheral blood in patients with rheumatoid arthritis. *Rheumatology International*. 2004;24(6):351-4.
22. Weng NP, Akbar AN, Goronzy J. CD28(-) T cells: their role in the age-associated decline of immune function. *Trends in Immunology*. 2009;30(7):306-12.
23. Broux B, Markovic-Plese S, Stinissen P, Hellings N. Pathogenic features of CD4(+)CD28(-) T cells in immune disorders. *Trends in Molecular Medicine*. 2012;18(8):446-53.
24. Warrington KJ, Vallejo AN, Weyand CM, Goronzy JJ. CD28 loss in senescent CD4+ T cells: reversal by interleukin-12 stimulation. *Blood*. 2003;101(9):3543-9.
25. Pinto-Medel MJ, Garcia-Leon JA, Oliver-Martos B, Lopez-Gomez C, Luque G, Arnaiz-Urrutia C, et al. The CD4(+) T-cell subset lacking expression of the CD28 costimulatory molecule is expanded and shows a higher activation state in multiple sclerosis. *Journal of Neuroimmunology*. 2012;243(1-2):1-11.
26. Nakajima T, Schulte S, Warrington KJ, Kopecky SL, Frye RL, Goronzy JJ, et al. T-cell-mediated lysis of endothelial cells in acute coronary syndromes. *Circulation*. 2002;105(5):570-5.
27. Hellings N, Broux B, Pannemans K, Zhang X, Markovic-Plese S, Broekmans T, et al. CX3CR1 DRIVES CD4+CD28NULL CYTOTOXIC T CELLS INTO THE CENTRAL NERVOUS SYSTEM OF MS PATIENTS. *Glia*. 2011;59:S139-S.

28. Thewissen M, Somers V, Heltings N, Stinissen P, Venken K. CD4+CD28null T cells in autoimmune disease: Pathogenic features and decreased susceptibility to immunoregulation. *Clinical Immunology*. 2007;123:S148-S.
29. van Leeuwen EMM, Remmerswaal EBM, Vossen MTM, Rowshani AT, Wertheim-van Dillen PME, van Lier RAW, et al. Emergence of a CD4(+)CD28(-) granzyme B+, cytomegalovirus-specific T cell subset after recovery of primary cytomegalovirus infection. *Journal of Immunology*. 2004;173(3):1834-41.
30. Link A, Selejan S, Hewera L, Walter F, Nickenig G, Bohm M. Rosuvastatin induces apoptosis in CD4(+)CD28(null) T cells in patients with acute coronary syndromes. *Clinical Research in Cardiology*. 2011;100(2):147-58.
31. Bryl E, Vallejo AN, Weyand CM, Goronzy JJ. Down-regulation of CD28 expression by TNF-alpha. *Journal of Immunology*. 2001;167(6):3231-8.
32. Pierer M, Rossol M, Kaltenhauser S, Arnold S, Hantzschel H, Baerwald C, et al. Clonal expansions in selected TCR BV families of rheumatoid arthritis patients are reduced by treatment with the TNF alpha inhibitors etanercept and infliximab. *Rheumatology International*. 2011;31(8):1023-9.
33. Bryl E, Vallejo AN, Matteson EL, Witkowski JM, Weyand CM, Goronzy JJ. Modulation of CD28 expression with anti-tumor necrosis factor alpha therapy in rheumatoid arthritis. *Arthritis and Rheumatism*. 2005;52(10):2996-3003.
34. Fletcher JM, Vukmanovic-Stejic M, Dunne PJ, Birch KE, Cook JE, Jackson SE, et al. Cytomegalovirus-specific CD4(+) T cells in healthy carriers are continuously driven to replicative exhaustion. *Journal of Immunology*. 2005;175(12):8218-25.
35. Pourgheysari B, Khan N, Best D, Bruton R, Nayak L, Moss PAH. The cytomegalovirus-specific CD4(+) T-cell response expands with age and markedly alters the CD4(+) T-cell repertoire. *Journal of Virology*. 2007;81(14):7759-65.
36. Kijpittayarit S, Eid AJ, Brown RA, Paya CV, Razonable RR. Relationship between toll-like receptor 2 polymorphism and cytomegalovirus disease after liver transplantation. *Clinical Infectious Diseases*. 2007;44(10):1315-20.
37. Kang SH, Abdel-Massih RC, Brown RA, Dierkhising RA, Kremers WK, Razonable RR. Homozygosity for the Toll-Like Receptor 2 R753Q Single-Nucleotide Polymorphism Is a Risk Factor for Cytomegalovirus Disease After Liver Transplantation. *Journal of Infectious Diseases*. 2012;205(4):639-46.
38. Shirts BH, Kim JJ, Reich S, Dickerson FB, Yolken RH, Devlin B, et al. Polymorphisms in MICB are associated with human herpes virus seropositivity and schizophrenia risk. *Schizophrenia Research*. 2007;94(1-3):342-53.
39. Schmidt D, Goronzy JJ, Weyand CM. CD4+ CD7- CD28- T cells are expanded in rheumatoid arthritis and are characterized by autoreactivity. *J Clin Invest*. 1996;97(9):2027-37.
40. Sun Z, Zhong W, Lu X, Shi B, Zhu Y, Chen L, et al. Association of Graves' disease and prevalence of circulating IFN-gamma-producing CD28(-) T cells. *J Clin Immunol*. 2008;28(5):464-72.
41. Liao W, Lin JX, Leonard WJ. IL-2 family cytokines: new insights into the complex roles of IL-2 as a broad regulator of T helper cell differentiation. *Current Opinion in Immunology*. 2011;23(5):598-604.
42. Fasth AE, Snir O, Johansson AA, Nordmark B, Rahbar A, af Klint E, et al. Skewed distribution of proinflammatory CD4(+)CD28(null) T cells in rheumatoid arthritis. *Arthritis Research & Therapy*. 2007;9(5):11.
43. Appay V, Zaunders JJ, Papagno L, Sutton J, Jaramillo A, Waters A, et al. Characterization of CD4(+) CTLs ex vivo. *Journal of Immunology*. 2002;168(11):5954-8.
44. Fritsch RD, Shen XL, Sims GP, Hathcock KS, Hodes RJ, Lipsky PE. Stepwise differentiation of CD4 memory T cells defined by expression of CCR7 and CD27. *Journal of Immunology*. 2005;175(10):6489-97.
45. Duftner C, DeJaco C, Hengster P, Bijuklic K, Joannidis M, Margreiter R, et al. Apoptotic Effects of Antilymphocyte Globulins on Human Pro-inflammatory CD4(+)CD28(-) T-cells. *Plos One*. 2012;7(3):10.
46. McKay FC, Swain LI, Schibeci SD, Rubio JP, Kilpatrick TJ, Heard RN, et al. CD127 immunophenotyping suggests altered CD4(+) T cell regulation in primary progressive multiple sclerosis. *Journal of Autoimmunity*. 2008;31(1):52-8.
47. Alonso-Arias R, Moro-Garcia MA, Vidal-Castineira JR, Solano-Jaurrieta JJ, Suarez-Garcia FM, Coto E, et al. IL-15 preferentially enhances functional properties and antigen-specific responses of CD4+CD28(null) compared to CD4+CD28+T cells. *Aging Cell*. 2011;10(5):844-52.
48. Miyazaki Y, Iwabuchi K, Kikuchi S, Fukazawa T, Niino M, Hirotsani M, et al. Expansion of CD4+CD28- T cells producing high levels of interferon- $\gamma$  in peripheral blood of patients with multiple sclerosis. *Mult Scler*. 2008;14(8):1044-55.

49. Bernstein HB, Plasterer MC, Schiff SE, Kitchen CM, Kitchen S, Zack JA. CD4 expression on activated NK cells: ligation of CD4 induces cytokine expression and cell migration. *J Immunol.* 2006;177(6):3669-76.
50. Sommers CL, Dejarnette JB, Huang K, Lee J, El-Khoury D, Shores EW, et al. Function of CD3 epsilon-mediated signals in T cell development. *J Exp Med.* 2000;192(6):913-19.
51. Abbas AK, Lichtman AH. *Basic Immunology: Functions and disorders of the immune system.* Philadelphia: Saunders Elsevier; 2011. 312 p.



## 10 Supplementary figures and tables

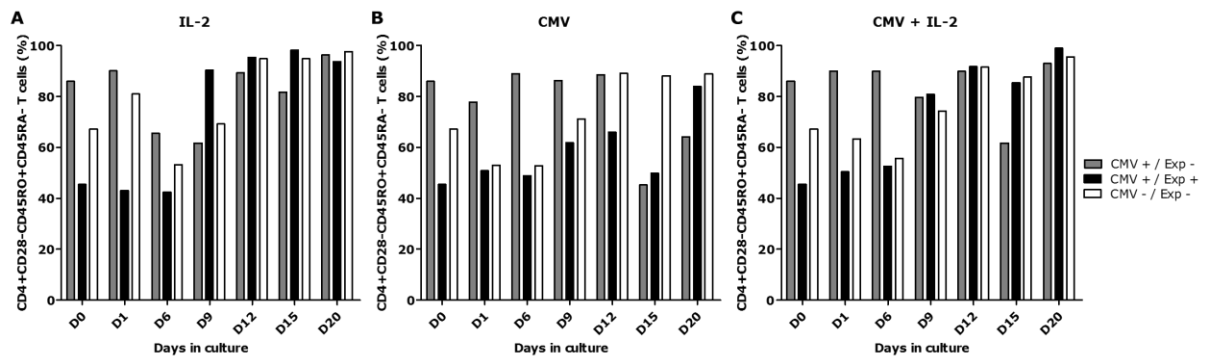


**Figure 1s: The percentage of CD4+CD28null CD45RO+CD45RA- T cells derived from 3 donors at different time points in a stimulatory environment.** PBMCs derived from 3 donors (CMV+/Exp+, CMV+/Exp-, and CMV-/Exp-) were cultured for maximum 20 days in (A) an IL-2, (B) a CMV, (C) a CMV+IL-2 stimulatory environment. At each time point PBMCs were analyzed with flow cytometry, and CD4+CD28null CD45RO+CD45RA- T cells were measured. PBMC: peripheral blood mononuclear cell; IL-2: interleukin-2; CMV: cytomegalovirus; CMV+/Exp+: cytomegalovirus seropositive and CD4+CD28null T cell expansion positive donor; CMV+/Exp-: cytomegalovirus seropositive and CD4+CD28null T cell expansion negative donor; CMV-/Exp-: cytomegalovirus seronegative and CD4+CD28null T cell expansion negative donor.

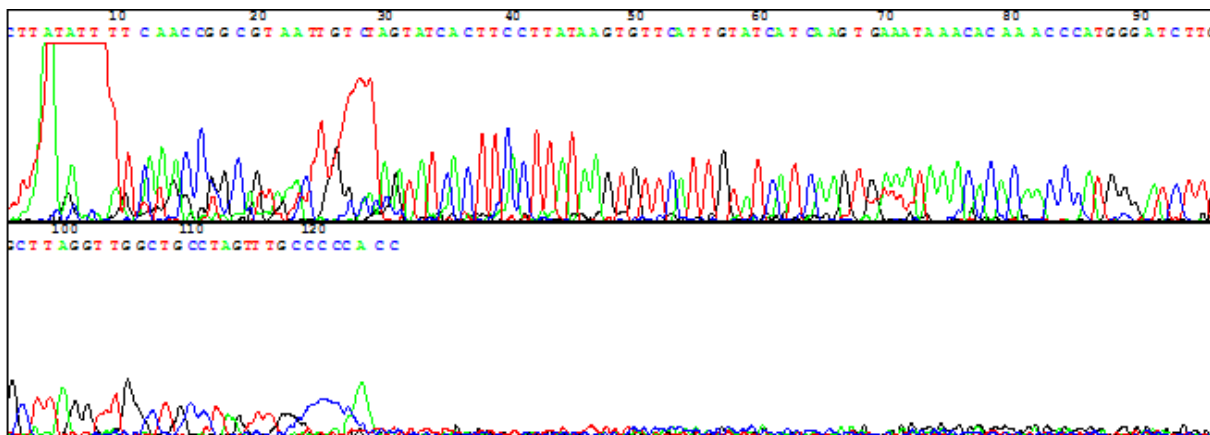


**Figure 2s: Sequencing result when the IFN- $\gamma$  reverse primer was used.**

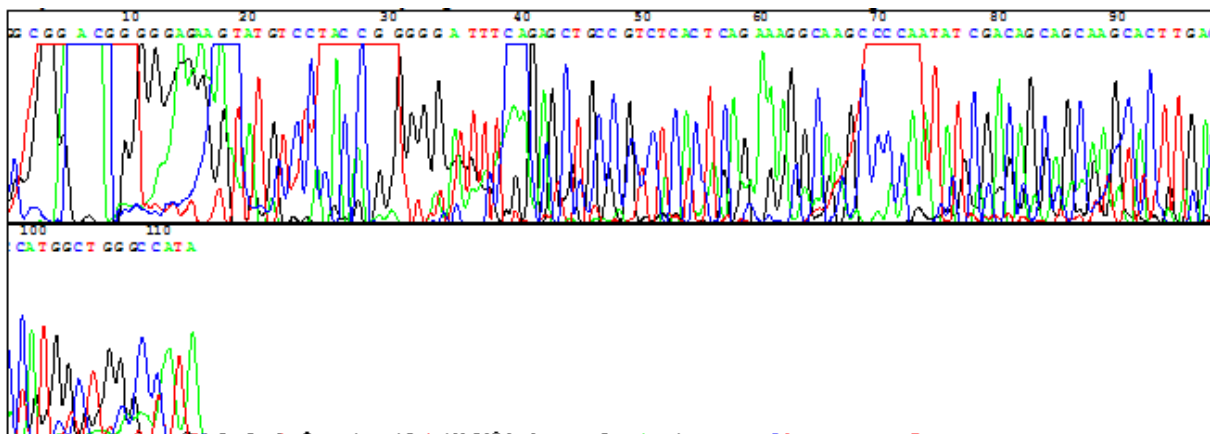


**Figure 3s: Sequencing result when the IL-17 reverse primer was used.**

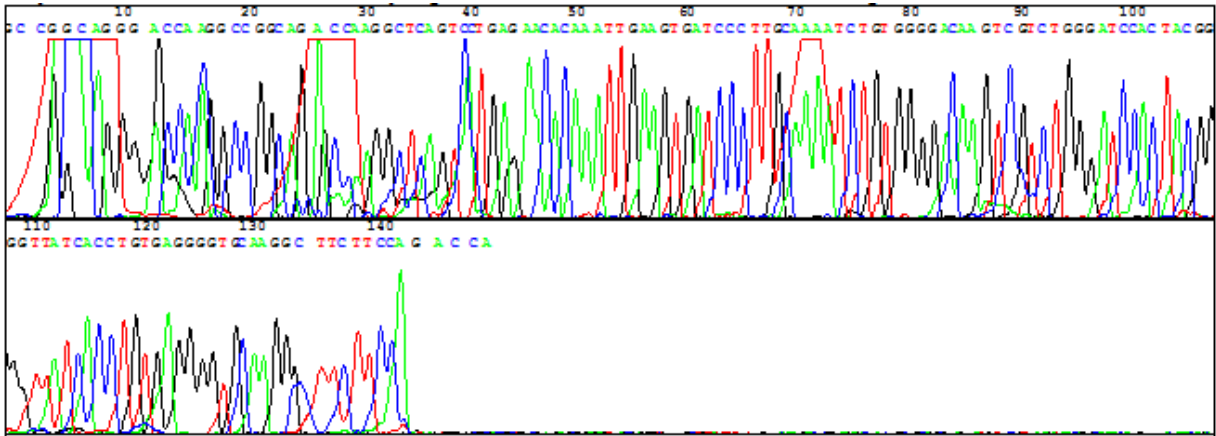


Figure 4s: Sequencing result when the RORyT forward primer was used.

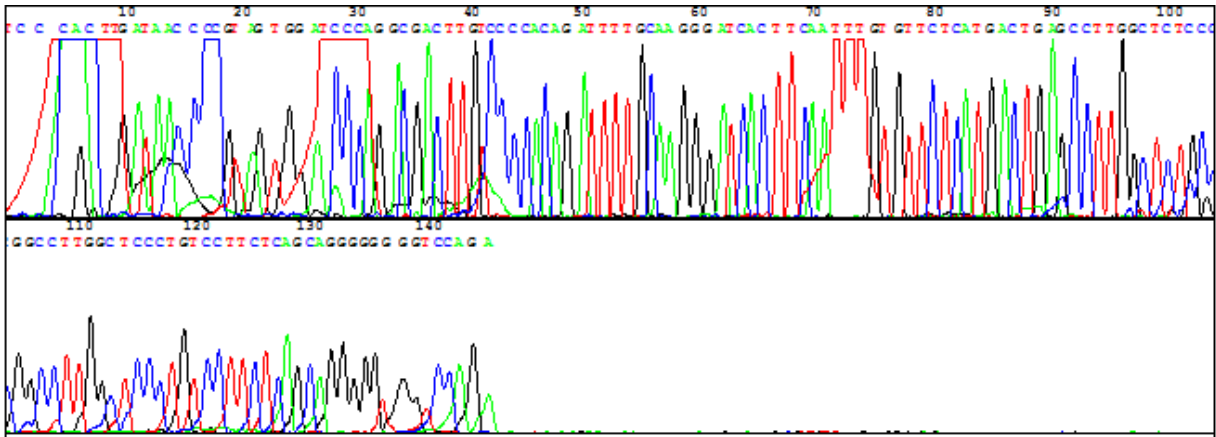


Figure 5s: Sequencing result when the RORyT reverse primer was used.

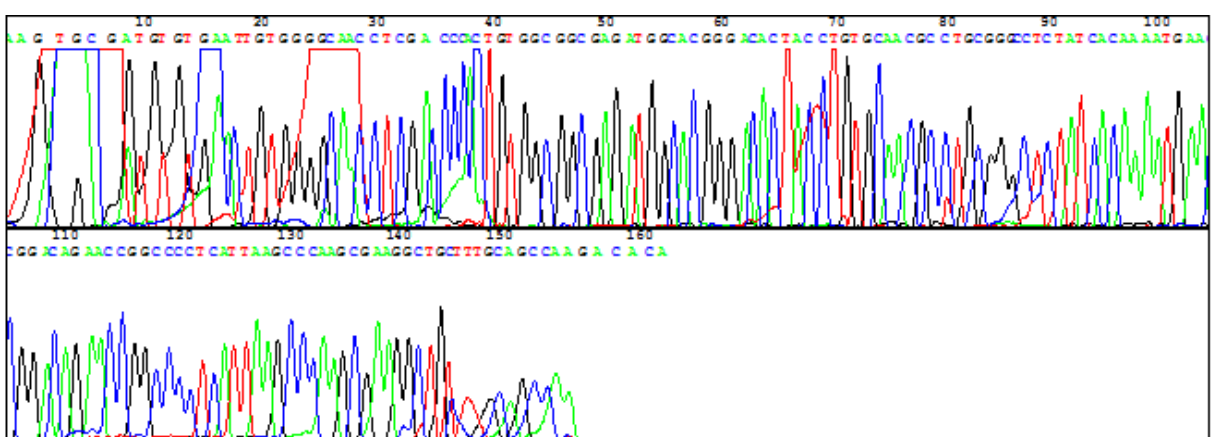


Figure 6s: Sequencing result when the GATA-3 forward primer was used.

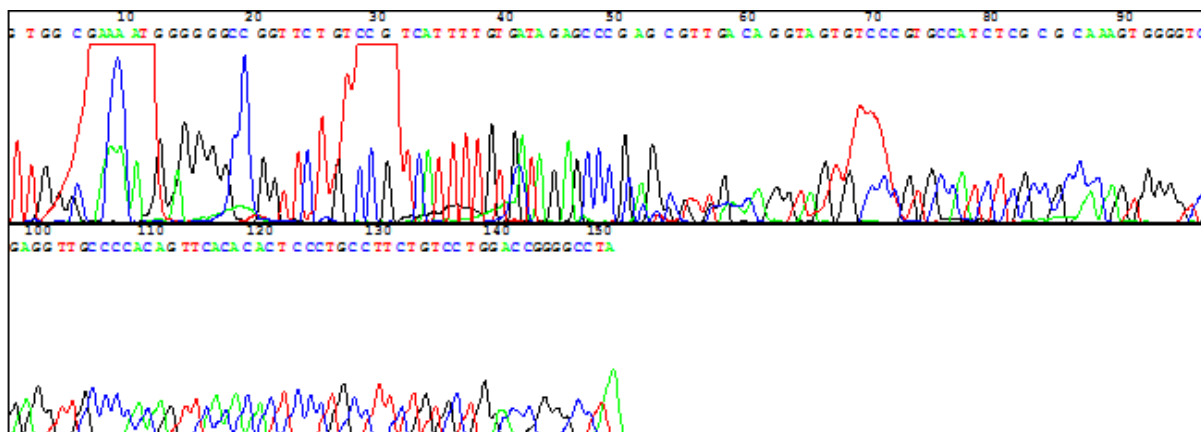


Figure 7s: Sequencing result when the GATA-3 reverse primer was used.

Table 1s: Alignment of sequencing result of IFN- $\gamma$ , IL-17, ROR $\gamma$ T and GATA-3 primers by performing a BLAST search

| Description  | Max score | Total score | Query cover | E value | Ident | Accession      |
|--|-----------|-------------|-------------|---------|-------|----------------|
| <b>IFN-<math>\gamma</math>, reverse primer</b>   |           |             |             |         |       |                |
| Homo sapiens interferon, gamma (IFNG), mRNA  | 178       | 178         | 94%         | 5e-44   | 93%   | NM_000619.2    |
| <b>IL-17, reverse primer</b>   |           |             |             |         |       |                |
| Homo sapiens interleukin 17F (IL17F), mRNA   | 143       | 143         | 86%         | 2e-33   | 93%   | NM_052872.3    |
| <b>ROR<math>\gamma</math>T, forward primer</b>   |           |             |             |         |       |                |
| Homo sapiens RAR-related orphan receptor C (RORC), transcript variant 2, mRNA                  | 230       | 230         | 92%         | 2e-59   | 97%   | NM_001001523.1 |
| Predicted: Homo sapiens RAR-related orphan receptor C (RORC), transcript variant X4, misc mRNA | 171       | 171         | 65%         | 1e-41   | 99%   | XR_426792.1    |
| Predicted: Homo sapiens RAR-related orphan receptor C (RORC), transcript variant X2, mRNA      | 171       | 171         | 65%         | 1e-41   | 99%   | XM_005245424.2 |
| Predicted: Homo sapiens RAR-related orphan receptor C (RORC), transcript variant X3, mRNA      | 171       | 171         | 65%         | 1e-41   | 99%   | XM_006711484.1 |
| Homo sapiens RAR-related orphan receptor C (RORC), transcript variant 1, mRNA                  | 171       | 171         | 65%         | 1e-41   | 99%   | NM_005060.3    |
| <b>ROR<math>\gamma</math>T, reverse primer</b>   |           |             |             |         |       |                |
| Homo sapiens RAR-related orphan receptor C (RORC), transcript variant 2, mRNA                  | 235       | 235         | 94%         | 4e-61   | 98%   | NM_001001523.1 |
| Predicted: Homo sapiens RAR-related orphan receptor C (RORC), transcript variant X4, misc mRNA | 122       | 122         | 47%         | 3e-27   | 99%   | XR_426792.1    |
| Predicted: Homo sapiens RAR-related orphan receptor C  | 122       | 122         | 47%         | 3e-27   | 99%   | XM_005245424.2 |

|   |     |     |     |       |     |                |  |
|---|-----|-----|-----|-------|-----|----------------|--|
| (RORC), transcript variant X2, mRNA   |     |     |     |       |     |                |  |
| Predicted: Homo sapiens RAR-related orphan receptor C (RORC), transcript variant X3, mRNA | 122 | 122 | 47% | 3e-27 | 99% | XM_006711484.1 |  |
| Homo sapiens RAR-related orphan receptor C (RORC), transcript variant 1, mRNA             | 122 | 122 | 47% | 3e-27 | 99% | NM_005060.3    |  |
| <b>GATA-3, forward primer</b>   |     |     |     |       |     |                |  |
| Predicted: Homo sapiens GATA binding protein 3 (GATA3), transcript variant X2, mRNA       | 241 | 241 | 90% | 9e-63 | 97% | XM_005252443.2 |  |
| Predicted: Homo sapiens GATA binding protein 3 (GATA3), transcript variant X1, mRNA       | 241 | 241 | 90% | 9e-63 | 97% | XM_005252442.1 |  |
| Homo sapiens GATA binding protein 3 (GATA3), transcript variant 1, mRNA                   | 241 | 241 | 90% | 9e-63 | 97% | NM_001002295.1 |  |
| Homo sapiens GATA binding protein 3 (GATA3), transcript variant 2, mRNA                   | 241 | 241 | 90% | 9e-63 | 97% | NM_002051.2    |  |
| <b>GATA-3, reverse primer</b>   |     |     |     |       |     |                |  |
| Predicted: Homo sapiens GATA binding protein 3 (GATA3), transcript variant X2, mRNA       | 209 | 209 | 94% | 2e-53 | 93% | XM_005252443.2 |  |
| Predicted: Homo sapiens GATA binding protein 3 (GATA3), transcript variant X1, mRNA       | 209 | 209 | 94% | 2e-53 | 93% | XM_005252442.1 |  |
| Homo sapiens GATA binding protein 3 (GATA3), transcript variant 1, mRNA                   | 209 | 209 | 94% | 2e-53 | 93% | NM_001002295.1 |  |
| Homo sapiens GATA binding protein 3 (GATA3), transcript variant 2, mRNA                   | 191 | 191 | 94% | 9e-48 | 91% | NM_002051.2    |  |

**Table 2s: EAE scoring system according to Hooke laboratories (EAE induction by active immunization in C57BL/6 mice)**

| <b>Score</b> | <b>Clinical observation</b>  |
|--------------|--|
| <b>0.0</b>   | No obvious changes in motor function compared to non-immunized mice.<br><br>When picked up by base of tail, the tail has tension and is erect. Hind legs are usually spread apart. When the mouse is walking, there is no gait or head tilting.  |
| <b>0.5</b>   | Tip of tail is limp.<br><br>When picked up by base of tail, the tail has tension except for the tip. Muscle straining is felt in the tail, while the tail continues to move.   |
| <b>1.0</b>   | Limp tail.<br><br>When picked up by base of tail, instead of being erect, the whole tail drapes over finger. Hind legs are usually spread apart. No signs of tail movement are observed.   |
| <b>1.5</b>   | Limp tail and hind leg inhibition.<br><br>When picked up by base of tail, the whole tail drapes over finger. When the mouse is dropped on a wire rack, at least one hind leg falls through consistently. Walking is very slightly wobbly.  |
| <b>2.0</b>   | Limp tail and weakness of hind legs.<br><br>When picked up by base of tail, the legs are not spread apart, but held closer together. When the mouse is observed walking, it has a clearly apparent wobbly walk. One foot may have toes dragging, but the other leg has no apparent inhibitions of movement.<br><br>OR<br><br>Mouse appears to be at score 0.0, but there are obvious signs of head tilting when the walk is observed. The balance is poor. |
| <b>2.5</b>   | Limp tail and dragging of hind legs.<br><br>Both hind legs have some movement, but both are dragging at the feet (mouse trips on hind feet).<br><br>OR<br><br>No movement in one leg/completely dragging one leg, but movement in the other leg.<br><br>OR<br><br>EAE severity appears mild when picked up (as score 0.0-1.5), but there is a strong head tilt that causes the mouse to occasionally fall over.  |
| <b>3.0</b>   | Limp tail and complete paralysis of hind legs (most common).<br><br>OR<br><br>Limp tail and almost complete paralysis of hind legs. One or both hind legs are able to paddle, but neither hind leg is able to move forward of the hind hip.<br><br>OR<br><br>Limp tail with paralysis of one front and one hind leg.<br><br>OR   |

ALL of:

- Severe head tilting,
- Walking only along the edges of the cage,
- Pushing against the cage wall,
- Spinning when picked up by base of tail.

**3.5** Limp tail and complete paralysis of hind legs.

Mouse is moving around the cage, but when placed on its side, is unable to right itself. Hind legs are together on one side of body.

OR

Mouse is moving around the cage, but the hind quarters are flat like a pancake, giving the appearance of a hump in the front quarters of the mouse.

**4.0** Limp tail, complete hind leg and partial front leg paralysis.

Mouse is minimally moving around the cage but appears alert and feeding. Often euthanasia is recommended after the mouse scores 4.0 for 2 days. However, with daily s.c. fluids some mice can recover to 3.5 or 3.0. When the mouse is euthanized because of severe paralysis, a score of 5.0 is entered for that mouse for the rest of the experiment.

**4.5** Complete hind and partial front leg paralysis, no movement around the cage. Mouse is not alert.

Mouse has minimal movement in the front legs. The mouse barely responds to contact. Euthanasia is recommended. When the mouse is euthanized because of severe paralysis, a score of 5.0 is entered for that mouse for the rest of the experiment.

**5.0** Mouse is spontaneously rolling in the cage (euthanasia is recommended).

OR

Mouse is found dead due to paralysis.

OR

Mouse is euthanized due to severe paralysis.

---

## Auteursrechtelijke overeenkomst

Ik/wij verlenen het wereldwijde auteursrecht voor de ingediende eindverhandeling:

**The immunological activity of CD4+CD28null T cells in the pathogenesis of multiple sclerosis**

Richting: **master in de biomedische wetenschappen-klinische moleculaire wetenschappen**

Jaar: **2014**

in alle mogelijke mediaformaten, - bestaande en in de toekomst te ontwikkelen - , aan de Universiteit Hasselt.

Niet tegenstaand deze toekenning van het auteursrecht aan de Universiteit Hasselt behoud ik als auteur het recht om de eindverhandeling, - in zijn geheel of gedeeltelijk -, vrij te reproduceren, (her)publiceren of distribueren zonder de toelating te moeten verkrijgen van de Universiteit Hasselt.

Ik bevestig dat de eindverhandeling mijn origineel werk is, en dat ik het recht heb om de rechten te verlenen die in deze overeenkomst worden beschreven. Ik verklaar tevens dat de eindverhandeling, naar mijn weten, het auteursrecht van anderen niet overtreedt.

Ik verklaar tevens dat ik voor het materiaal in de eindverhandeling dat beschermd wordt door het auteursrecht, de nodige toelatingen heb verkregen zodat ik deze ook aan de Universiteit Hasselt kan overdragen en dat dit duidelijk in de tekst en inhoud van de eindverhandeling werd genotificeerd.

Universiteit Hasselt zal mij als auteur(s) van de eindverhandeling identificeren en zal geen wijzigingen aanbrengen aan de eindverhandeling, uitgezonderd deze toegelaten door deze overeenkomst.

Voor akkoord,

**Peters, Michiel**

Datum: **10/06/2014**